February 22, 1991

Annual Report

Grant No. NAGW-319 Basic
15 January 1990 to 14 January 1991

PHOTOABSORPTION AND PHOTODISSOCIATION OF MOLECULES IMPORTANT IN THE INTERSTELLAR MEDIUM

Submitted by:

Long C. Lee and Masako Suto
Department of Electrical and Computer Engineering
San Diego State University
San Diego, California 92182

Prepared for :

NASA Headquarters
Washington, DC 20546

Attention: Dr. Lawrence J. Caroff
Astrophysics Division
Code EZ

Table of Contents

I. Introduction

The photoabsorption, photodissociation, and fluorescence cross sections of interstellar molecules are measured at 90-250 nm. These quantitative optical data are needed for the understanding of the formation and destruction processes of molecules under the intense interstellar UV radiation field. The experimental data for the molecules, NO, CH_4, CH_3OH, CH_3SH, and small aromatic molecules were measured in the reporting period.

The research effect in the current reporting period has been shifted to the observation of IR emissions from UV excitation of aromatic molecules. The research results are currently needed to study the sources for the "unidentified" interstellar infrared (UIR) emission bands. The IR emissions at 3.2-3.6 μm were observed from UV excitation of several aromatic molecules in the gas phase. The results lend a support to the model that polycyclic aromatic hydrocarbon (PAH) molecules are responsible for the UIR bands. The UIR band at 3.3 μm is likely due to the aromatic C-H stretching vibrational modes, and the UIR bands at 3.4-3.6 μm that usually accompany the 3.3 μm band are associated with the CH_3 groups in the methyl-derivatives of PAH molecules.

II. Research Accomplished

The research results accomplished in the period from January 15, 1990 to January 14, 1991 are summarized below:

A. Fluorescences from Photoexcitation of CH_4, CH_3OH, and CH_3SH

The photoabsorption and fluorescence cross sections of CH_4, CH_3OH, and CH_3SH were measured in the 50-106 nm region using synchrotron radiation as a light source. The optical emissions from photodissociative excitation of these molecules were dispersed, and the emitting species were identified by

the fluorescence spectra. Emissions from the excited H^* and CH^* are commonly observed from all three molecules studied. Additional emissions are observed from the excited CH_2^* by photoexcitation of CH_4, OH^* by CH_3OH, and CS^* by CH_3SH. Since these molecules are abundant in the interstellar medium, the current results are useful for the study of their photochemistry in the space. The results were summarized in a paper that was published in the Journal of Quantitative Spectroscopy and Radiative Transfer. The paper is attached as Appendix A.

B. NO γ Emission from Photoexcitation of NO

The photoabsorption cross section of NO was measured in the 50-120 nm region using synchrotron radiation as a light source. UV Emission was observed at the excitation wavelengths shorter than 79 nm. The emission was identified as the NO γ band that is produced from the $NO^+(a)$ + NO reaction. $NO^+(a)$ is produced by photoionization of NO. The result is summarized in a paper published in Chemical Physics Letters that is attached as Appendix B.

C. Photoexcitation Cross Sections of Aromatic Molecules

Large PAH molecules could be responsible for the UIR emission bands. The photoabsorption cross sections of the PAH molecules are needed for the calculation of their formation and destruction rates in the interstellar medium. Since large molecules are synthesized from small ones, small aromatic molecules may also exist in the interstellar medium. We start to measure the photoabsorption and photodissociation of small aromatic molecules in the current funding period using synchrotron radiation as a light source. The results for the absorption and fluorescence cross sections of benzene, xylenes, and naphthalene measured at 106-280 nm are summarized in a paper attached as Appendix C. The experimental results need to be confirmed because

the samples may contain impurities. Once the results are confirmed, we will submit the paper to scientific journal for publication.

D. **IR Emission from UV Excitation of $HONO_2$**

This research program started to observe IR emissions from UV excitation of interstellar molecules in the current reporting period. Because the IR emission from UV excitation of $HONO_2$ is known in literature, we chose this molecule to test our apparatus. The emission was dispersed and identified as the emission system of excited NO_2^*. The absolute cross section of the IR emission was measured at 0.8- 2.0 μm. The result was summarized in a paper that was published in the Journal of Quantitative Spectroscopy and Radiative Transfer. The paper is attached as Appendix D.

The $HONO_2$ result showed that our apparatus was suitable for observing IR emissions from UV excitation of PAH molecules.

E. **IR Emission from UV Excitation of Benzene and Methyl-Derivatives**

IR emissions from UV excitation of benzene, toluene, xylenes, mesitylene, and durene were observed in the 3.1-3.8 μm region. ArF excimer laser photons at 193 nm were used as the excitation light source. The emissions were dispersed to identify the emission system. An emission band with peak at 3.3 μm is commonly observed from all the molecules studied. The emission band is attributed to the $v = 1 \rightarrow 0$ transition of the aromatic C-H stretching vibrational modes. In addition to the 3.3 μm band, an emission band with peak at 3.43 μm is observed from the methyl-derivatives that is attributed to the C-H stretching vibrational modes of the CH_3 groups. This assignment is supported by the observation that the 3.43 μm emission intensity increases with the number of the CH_3 groups in the methyl-derivatives. The results are summarized in a paper attached as Appendix E. This paper has been submitted

to Chemical Physics Letters for publication.

The current results indicate that the UIR band at 3.3 μm is likely corresponding to the aromatic C-H stretching vibrational modes, and the 3.4-3.6 μm bands that usually accompany the 3.3 μm band are likely associated with the CH_3 groups.

F. IR Emission from UV Excitation of PAH Molecules

The IR emissions from UV excitation of PAH molecules such as naphthalene, phenanthrene, anthracene, pyrene, and their methyl-derivatives in the gas phase were observed. The ArF laser photons at 193 nm were used as the excitation light source. Similar to benzene and its methyl-derivatives, the 3.3 μm band is commonly observed from all the PAH molecules and additional bands in the 3.4-3.6 μm region are observed from the methyl-derivatives. Again, the 3.3 μm band is attributed to the aromatic C-H vibrational modes, and the 3.4-3.6 μm band to the vibrational modes of the CH_3 groups. The results are summarized in a paper attached as Appendix F. This paper has been submitted to Astrophysical Journal for publication.

The observed spectra are compared with the IR emissions universally observed in many astronomical objects. The current spectra are very similar to the UIR emission bands as shown in Fig.5 in Appendix F. The current laboratory data lend a support to the model that the "unidentified" interstellar IR emissions are due to PAH molecules.

The IR emissions from the 193 nm excitation of many interstellar molecules other than PAHs are also observed to compare with the interstellar IR emissions. The spectra from the non-PAH molecules are quite different from the UIR bands; thus, the non-PAHs are not responsible for the UIR bands.

III. Publications and Presentations in the Reporting Period

1. "Fluorescence from Excitation of CH_4, CH_3OH, and CH_3SH by Extreme Vacuum Ultraviolet Radiation", G. Ma, M. Suto, and L. C. Lee, J. Quant. Spectrosc. Radiat. Transfer, 44, 379 (1990).
2. "Infrared Emission from Dissociative Excitation of $HONO_2$ at 193 nm", J. Shan, M. Suto, and L. C. Lee, J. Quant. Spectrosc. Radiat. Transfer, in 45, 139 (1991).
3. "NO(γ) Emission by Energy Transfer from NO^+(a) to NO", G. Ma, M. Suto, and L. C. Lee, Chem. Phys. Lett. **176**, 141 (1991).
4. "Infrared Emission from UV Excitation of Benzene and Methyl-Derivatives", J. Shan, M. Suto, and L. C. Lee, submitted to Chem. Phys. Lett. for publication (1991).
5. "3.3 μm Emission from UV Excitation of Some Aromatic Molecules", J. Shan, M. Suto, and L. C. Lee, submitted to Astrophys. J. for publication.
6. "Fluorescences from Excited Photofragments", L. C. Lee and M. Suto, presented at the 1990 Annual Meeting of the Division of Atomic, Molecular, and Optical Physics of the American Physical Society, Monterey, CA, May 21-23, 1990.
7. "Emissions of Cl_2^* and NO^* Produced by Energy Transfer from Excited Photofragments", G. Ma, M. Suto, and L. C. Lee, presented at the XIXth Informal Conference on Photochemistry, University of Michigan, Ann Arbor, June 25-29, 1990.

IV. Appendices

A. "Fluorescence from Excitation of CH_4, CH_3OH and CH_3SH by Extreme Vacuum Ultraviolet Radiation"

B. "NO(γ) Emission by Energy Transfer from $NO^+(a)$ to NO"

C. "Photoexcitation and Fluorescence Cross Sections of Small Aromatic Molecules in the Gas Phase at 106-280 nm"

D. "Infrared Emission from Dissociative Excitation of $HONO_2$ at 193 nm"

E. "Infrared Emission from UV Excitation of Benzene and Methyl-Derivatives"

F. "3.3 μm Emission from UV Excitation of Some Aromatic Molecules"

Appendix C

Photoabsorption and Fluorescence Cross Sections of Small Aromatic Molecules in the Gas Phase at 106-280 nm

Masako Suto, Jun Shan, and L. C. Lee

Molecular Engineering Laboratory

Department of Electrical and Molecular Engineering

San Diego State University

San Diego, California 92182

ABSTRACT

Photoabsorption and fluorescence cross sections of benzene, xylenes, and naphthalene in the gas phase are measured in the 106-280 nm region using synchrotron radiation as a light source. All the molecules studied show fluorescence in the 220-290 nm region. The absolute fluorescence cross sections are measured by calibrating the fluorescence intensity with the NO(A, $v' = 2 \rightarrow X$, v'') emission system, for which the fluorescence yield is unity. The quantum yield of the $SO_2(\tilde{B} \rightarrow \tilde{X})$ emission system is measured to cross-check the current measurement technique. The fluorescence quantum yields are determined from the ratios of the fluorescence to the absorption cross sections, and the results are compared with previous values measured by different methods.

I. INTRODUCTION

The photoexcitation processes of small aromatic compounds have been extensively investigated. Benzene is one of the polyatomic molecules most frequently used as examples for both experimental and theoretical studies. The photoabsorption cross sections of benzene have been measured at 135-295 nm, [1-3] and the fluorescence quantum yields have also been determined at 200-250 nm.[4-6] There are many studies for the radiative and non-radiative decay processes of the electronically-excited states of benzene[7]. Among the aromatic molecules, the absorption and fluorescence data of benzene are the most extensively documented.

All three isomers of dimethyl-benzene (meta-, ortho- and para-xylene) fluoresce in the UV region, and their fluorescence quantum yields were determined both in the gas phase[8] and in solutions[9]. The absorption spectra of xylenes in the vacuum UV region were measured in the gas phase,[10-12] in liquid solutions,[13,14] and in rare gas matrix.[15] The photoexcitation processes of xylenes are not as well studied as benzene. The absorption and fluorescence cross sections of gaseous xylenes that are of interest for the study of their excited states are expected to be similar to those of benzene.

The absorption spectrum of naphthalene vapor was measured at 40-330 nm by several groups.[10,16-20] Koch et al.[20] reported the absorption spectrum from 5 to 30 eV using synchrotron radiation as a light source. The absorption cross section (or molar extinction coefficient) was measured by Kitagawa[16] and by Morris's group[17,18] in the 143-330 nm region. Fluorescence from the singlet states in the UV region is of interest for the study of radiative and non-radiative processes in parallel to benzene. Stockburger et al[21] measured the fluorescence quantum yields for a number of single vibronic levels.

In the current experiment, the photoabsorption cross sections of benzene,

xylenes, and naphthalene in the gas phase are measured 106-280 nm using synchrotron radiation as a light source. All molecules show fluorescence at 220-290 nm, but not in the wavelengths shorter than 220 nm. The absolute fluorescence cross sections are obtained by calibrating the fluorescence intensity with the NO($A \rightarrow X$) and $SO_2(\tilde{B} \rightarrow \tilde{X})$ emission systems, for which the fluorescence yields are close to 1. The current data are useful for the modeling of the abundance of these aromatic molecules in the interstellar medium.

II. EXPERIMENTAL

The experimental setup has been described in previous papers.[22] In Brief, synchrotron radiation produced from the 1-GeV electron storage ring at the University of Wisconsin was dispersed by a 1-m vacuum monochromator (Seya-Namioka type). A LiF window was used to separate the gas cell from the high vacuum monochromator. The light source passed through the gas cell was converted to visible light by sodium salycilate coated on a glass window and detected by a photomultiplier tube (PMT, EMI 9558B) sensitive for $\lambda > 300$ μm. The optical path length of the absorption cell was 40.7 cm. Absorption cross sections were determined in accordance to Beer's law. The absorbance depends linearly on gas pressure, and the absorption cross section is determined from the slope of the linear plot of absorbance versus pressure. It is noted that the peak cross section and the bandwidth for a sharp band depend on the slit width of the monochromator. The UV-visible fluorescence was monitored by a cooled PMT (EMI 9558QB) sensitive in the 190-800 nm region. The fluorescence intensity was simultaneously observed with the photoabsorption measurement in a direction perpendicular to the light source beam.

Samples were supplied by Aldrich with stated purities better than 99.0% for p-xylene, m-xylene and o-xylene, 99.99% for benzene, and 99% for

naphthalene. Each sample was kept in a stainless steel container and degassed at the liquid nitrogen temperature prior to use for experiment. Precaution was taken for m-xylene to avoid oxidation by ambient air. NO(99.0%) and SO_2(99.9%) were obtained from both Matheson and Aldrich. They were used without further purification. The gas cell was continuously pumped by a sorption pump. The pressure in the gas cell was monitored by a capacitance manometer.

III. Data Analysis

The fluorescence intensity is given by,

$$I_f = CF\sigma_f n I_o \exp(-\sigma n l)/(1 + \tau k n) \qquad (1)$$

where C is a geometrical constant, F the PMT detection efficiency, l(~7.4 cm) the optical path length from the LiF window to the center of the PMT view region, σ_f the fluorescence cross section, n the gas density, I_o the light source intensity without sample gas, σ the absorption cross section, τ the radiative lifetime of the excited species, and k the quenching rate constant of the excited species by the gas in the gas cell.

If the sample pressure is low, (1) is reduced to,

$$I_f = CF\sigma_f n I_o \qquad (2)$$

The constant CF can be determined by compareing to a reference gas with known fluorescence cross section if both the fluorescence intensities of the sample gas and the reference gas are measured in the same experimental setup. Once the constant is determined, σ_f can be obtained from the fluorescence intensity.

The 2-0 band of the NO($A^2\Sigma^+ - X^2\Pi$) transition at 204-206 nm was used as the calibration standard for the fluorescence cross section measurement. The quantitative spectroscopic data of the NO γ band are well established.[23]

The fluorescence yield of the 2-0 band is assumed to be unity, because the NO(A, v = 2) level is below the dissociation limit of NO, so it decays only by radiation to the ground state. Thus, the fluorescence cross section is equal to the absorption cross section. The fluorescence of the NO γ (2 → v″) bands is in the 204-300 nm region. The efficiency of the PMT in this wavelength region is almost constant (within ± 10%).

To cross-check our calibration method, the quantum yield for fluorescence from photoexcitation of SO_2 was measured in this experiment using the NO γ fluorescence as a standard. SO_2 has two absorption systems, α_1 and α_2, in the 180-235 nm region. These systems emit resonance fluorescence that extends from the excitation wavelength to 430 nm with a broad maximum at about 320 nm.[24] SO_2 starts to predissociate at 220 nm where the fluorescence yield decreases abruptly.[24] Using the NO as a standard, the absorption and fluorescence cross sections of SO_2 were measured. The quantum yields of SO_2 at various excitation wavelengths were determined by the ratios of the fluorescence to the absorption cross sections. As expected, the fluorescence yields for excitation wavelengths longer than 224 nm are nearly unity. Hui and Rice[25] have measured SO_2 fluorescence yields by using fluorescence yields of 0.27 for benzene $^1B_{2u}(6_0^1)$ at 259 nm[26] as a standard. Their raw values of the quantum yields for SO_2 exceeded unity by 13 %. They attributed it to the experimental uncertainty and normalized the value at 227.7 nm to unity. The current measurements agree with their results within experimental uncertainties. The uncertainty in the current measurement is estimated to be within 10% of the given value.

The fluorescence quantum yield of benzene was measured using the same method. It is found that the quantum yields of benzene is about 10-13%, which is lower than the presently accepted values. Detail for the comparison is

discussed later in this paper.

IV. RESULTS AND DISCUSSION

1. Benzene and Xylenes

1.1 Absorption Cross Sections

The absorption cross sections of (a) benzene, (b) p-xylene, (c) o-xylene, and (d) m-xylene at 106-220 nm are shown in Fig.1. The spectral resolution is 0.1 nm and experimental uncertainty is ± 15% of the given value. The absorption cross section of benzene has been measured by Pantos et al.[3] at 4.2-9.2 eV (135-295 nm). They normalized the uncalibrated absorption spectrum obtained by Koch and Otto[2] at 6-36 eV with their values and calculated the absorption cross section and the oscillator strength at 4.2-36 eV. The absorption cross sections measured in this study agree with their values within experimental uncertainty.

The absorption spectra of benzene derivatives are usually discussed in analogy with the spectrum of benzene. In general, the substitution of alkyl groups in benzene shifts the absorption bands to longer wavelengths and broadens the bandwidths as well. The substitution has an effect on the absorption bands of Rydberg transition.[1] These effects are readily shown in Fig.1, where the wavelengths of corresponding transitions are red-shifted and the Rydberg absorption bands are broadened for xylenes. The absorption spectra of xylenes in the gas phase were reported by Hammond et al.[10] at 120-220 nm, but the absolute cross sections were not given. Prominent features shown in the current absorption spectra are in a good agreement with those previous spectra, but most of the weak structures were not in the earlier data.

As seen in Fig.1, the absorption spectra show a broad and continuum -like

absorption band starting around 220 nm and reaching a strong peak around 185 nm. This strong absorption band corresponds to the $^1E_{1u} \leftarrow {}^1A_{1g}$ transition of benzene at 6.9 eV. According to the assignment by Koch and Otto[2], a number of sharp bands for benzene at 134-153 nm is the Rydberg transitions converging to the first ionization potential at 9.27 eV (134.8 nm). Several sharp peaks superimposed on the strong broad band at 160- 185 nm are assigned to the early members of Rydberg series.

The first ionization potentials of xylenes are considerably lower than that of benzene, which are 8.56 eV (144.8 nm) for o- and m-xylenes and 8.44 (146.9 nm) for p-xylene. Thus, the Rydberg transitions are expected to shift to the longer wavelengths than that of benzene. The Rydberg series are observed at 145-170 nm. Weak structures superimposing on the strong absorption band at 180-196 nm could also be assigned to the early members of Rydberg series in analogy to benzene. In the wavelength region shorter than the first ionization potential, the weak structures could be assigned to the Rydberg series converging to the high ionization states.

The absorption cross sections of benzene and xylenes at 220-280 nm are shown in Fig.2. The spectral resolution was 0.1 nm, and the experimental uncertainty was ±15 % of the given values. The absorption spectrum of benzene consists of a number of sharp vibronic bands. The absorption cross section in this region strongly depends on instrumental bandwidth; that is, the higher the resolution, the larger is the peak value. Pantos et al.[3] have measured the gas phase cross section at three different bandwidths. The current cross section measured at the bandwidth of 0.1 nm is slightly lower than those measured by Pantos et al.[3] with a bandwidth of 0.008 nm. These results are considered to be in good agreement.

The absorption bands of xylenes are broader and shifted to the longer

wavelength than benzene as shown in Fig.2. The absorption spectra of xylenes in the gas phase were photographed and analyzed by Cooper et al.[11,12] at 235-285 nm. Our spectra are very close to theirs. The molar extinction coefficient of p-xylene in hexene solution was reported by Kato et al.[14] at 180-283 nm. Strong absorption peaks are recognized from their spectra, which show peaks shifted to the longer wavelengths. The absorption spectra of p- and m-xylenes were measured in Kr matrix at 185-280 nm.[13] Strong absorption peaks were observed at the slightly longer wavelengths, where some additional structures are attributed to different trapping sites in the matrix.

1.2. Fluorescence Cross Sections and Quantum Yields

No fluorescences were observed from photoexcitation of benzene and xylenes at 106-220 nm. In this wavelength region, small aromatic molecules may undergo (pre-)dissociation.[27] In the 250-280 nm region, the molecules fluoresce, and their quantum yields were measured. Several discrete absorption bands of benzene at 230-260 nm are assigned to the first singlet excited state. The fluorescence cross section observed with same spectral resolution is shown by the dotted line in Fig.2(a).

The fluorescence spectrum of benzene extends from the excitation wavelength to 350 nm. This wavelength region is very close to the fluorescence spectra of NO and SO_2 used as standard. Therefore, the error due to the PMT response would be negligibly small (< 5%). The other possible error is due to the light source intensity measurement. The incident light was converted into visible light by sodium salicylate coated on a glass window, which was measured by a PMT (EMI 9885B). No light shorter than 300 nm can transmit through the window. The efficiency of sodium salicylate in the 200-350 nm region was measured to be constant.[28] The uncertainty due to the VUV light conversion may be small (<5%). However, the stray light that

could accompany with the principle light may cause a large uncertainty that could as high as 15%. Since the band structure is so sharp, and the monochromator resolution is not high enough to resolve each single vibronic levels, the calculation of the quantum yield by the ratio of the absorption to the fluorescence cross sections may introduce a large error that could be as high as 20%. The overall experimental uncertainty is estimated to be ± 30% of the given value. The quantum yield of 10-13 % for the 6_0^1 level determined in the current measurement is lower than the values of 18% or 27 % generally adopted in the literature.[4-6]

The fluorescence quantum yield of benzene has been measured by two independent methods. Ishikawa et al.[4] and Poole[5] used the biacetyl method to measure the quantum yield to be 0.23. Noyes et al.[6] have determined quantum yield with well defined gas chamber. They critically reviewed previous values including their latest value and concluded that the quantum yield at 253.7 nm was 0.18 ± 0.04 for benzene pressure of 0.1 to 10 Torr. Since then, the yield of 0.18 is generally accepted as a standard, for example, Parmenter and Schuyler[26] based on the value to determine the yields for three single vibronic levels (SVL) of benzene, and Spear and Rice[29] extended the quantum yield measurement to a number of other SVL based on the Parmenter and Schuyler's values. The later studies on fluorescence quantum yields, triplet excitation, intersystem crossing, and channel three nonradiative decay are all based on the quantum yield of 0.18 or 0.27. The current result indicates that the quantum yield could be lower than the accepted value, although the uncertainties in the current and earlier experiments could make an amicable agreement. This difference is subject to further investigation.

The fluorescence cross sections of xylenes are shown in Figs.2 (b)-(d). Many vibrational structures are related to those shown in the absorption cross

sections. The fluorescence quantum yields obtained from the ratio of fluorescence to the absorption cross sections are a smooth function of the excitation wavelengths. The quantum yields of xylenes are shown in Fig.3. As listed in Table 1, the maximum yields are 22, 15 and 15% for p-, o-, and m-xylene, respectively. The experimental uncertainty is estimated to be ±30% of the given values. These values are lower than those measured previously using benzene as a standard.

The fluorescence spectra from xylenes were studied in our laboratory using KrF laser as a light source. The spectra show very broad emission bands at 260-350 nm with a broad maximum at 290 nm. These spectra are very similar to those observed in the liquid phase.[9] The PMT response for the fluorescences observed in xylenes is almost the same as those of NO and SO_2. The uncertainty caused by the PMT response is expected to be small.

2. Naphthalene

The absorption cross section of naphthalene was measured with spectral resolution of 0.1 nm. The results are shown in Fig. 4 and 5 for the regions of 106-230 and 230-290 nm, respectively. The absorption spectrum at 106-290 nm has been studied by many groups.[16-21] The molar extinction coefficients at 189-330 nm were measured by Morris and co-workers.[17,18] Our absorption cross section are in good agreement with their values in the overlapped wavelength region. There is no absorption cross section data available for the wavelengths shorter than 143 nm.

The absorption bands of naphthalene have been assigned[19,20] to a number of valence states (π^*-π transition) and Rydberg states. The first excited singlet state, S_1, extends above 283 nm, which is not included in present study. The absorption at 230-280 nm is due to the transition to the second singlet levels, S_2. The absorption to third singlet state is very strong that

is at 180-230 nm. These excited singlet states fluoresce.

In the 155-230 nm region, there are a number of bands superimposed on a continuum. Koch et al.[20] assigned most of them to the Rydgerg series converging to the first and higher ionization limits at 8.15, 8.90, 10.00, and 11.05 eV. Underlying continua could be the π^*-π transitions.[19] The peculiar absorption profile at 152-172 nm is similar to the "antiresonance" profile that is often observed in autoionization process. The antiresonance has been attributed[19] to the interference effect between Rydberg states and the π^* state.

The fluorescence from the vibrational levels of the S_1 state of naphthalene has been extensively investigated.[30] The fluorescence spectra from the vibrational levels of the S_2 and S_3 states are almost identical to that of the S_1 state. This similarity could be due to very fast internal conversion from S_2 and S_3 states to the higher vibronic levels of the S_1 state. The conversion rate could be much faster than the S_2 and S_3 radiative rates so that no direct fluorescence from the S_2 and S_3 states could be observed. The fluorescence quantum yield of the S_2 state relative to that of the S_1 state is about 0.06% when naphthalene is excited at 265.4 nm.[30] This small yield may be due to strong coupling between the isoenergetic vibronic levels in both the S_1 and S_2 states.

The fluorescence cross section of naphthalene measured by using NO emission as a calibration standard is shown in Fig.5(a). The S_1 fluorescence spectrum extends from 300 to 400 nm,[9] which is in the same wavelength regions of the NO and SO_2 fluorescence. The correction for the PMT efficiency is not needed. The quantum yield determined from the ratio of the fluorescence and the absorption cross sections is shown in Fig.5(b). The quantum yield has been measured by Stochburger et al.[21] The current results are about 30% lower

Table I--The ratios of the emission intensity to the number of the CH_3 groups in benzene methyl-derivatives.

Chemical	A*	B**	A/B
Toluene	0.167	0.2	0.84
o-Xylene	0.455	0.5	0.91
m-Xylene	0.386	0.5	0.77
p-Xylene	0.417	0.5	0.83
Mesitylene	0.670	1.0	0.67
Durene	1.156	2.0	0.58

* A is the intensity ratio of the 3.43 μm band to the 3.3 μm band.

** B is the ratio of the number of the CH_3 groups to the number of the H atoms bonded on the ring.

Figure Caption

Fig.1 IR emission spectra observed from photoexcitation of (a) benzene and (b) toluene at 193 nm. The spectral resolution is 0.025 μm. The dashed line in (a) shows the response of the detection system. The dashed line in (b) shows the extension of the 3.3 μm band. The dash-dot line in (b) shows the 3.43 μm band.

Fig.2 (a) IR emission spectra observed from the 193 nm excitation of benzene at the laser powers and the gas pressures of (1) 35 mJ/pulse and 1.7 Torr, (2) 10 mJ/pulse and 1.7 Torr, and (3) 18 mJ/pulse and 0.4 Torr. (b) The dependence of IR emission intensity on laser power observed at the emission wavelengths 3.1 μm (triangle) and 3.3 μm (dot).

Fig.3 IR emission spectra from photoexcitation of (a) o-xylene, (b) m-xylene, and (c) p-xylene at 193 nm. The spectral resolution and notations are same as Fig.1.

Fig.4 IR emission spectra from photoexcitation of mesitylene and durene at 193 nm. The spectral resolution and notations are same as Fig.1.

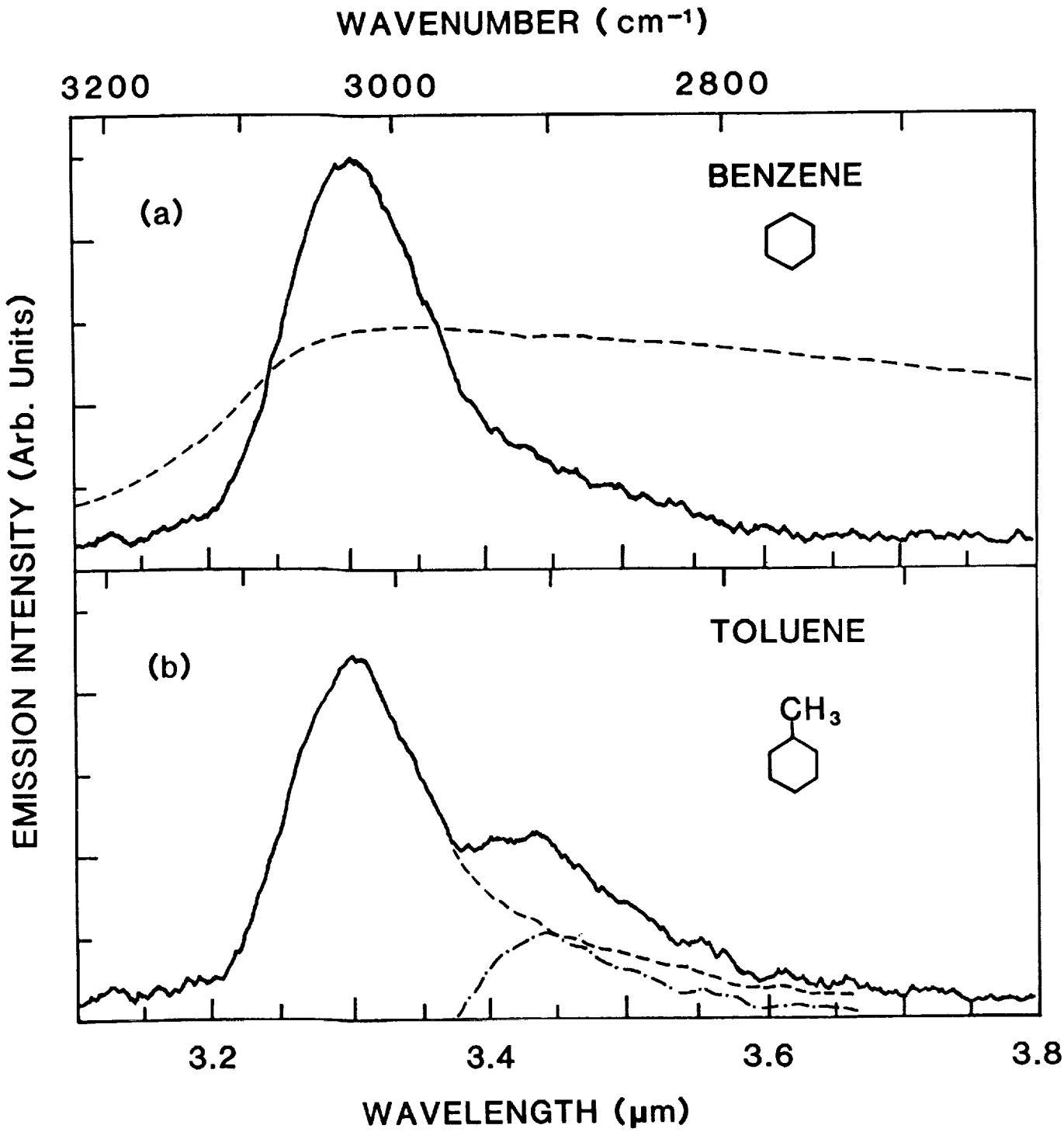
WAVENUMBER (cm⁻¹)
3200
3000
2800
(a)
BENZENE
(b)
TOLUENE
CH3
EMISSION INTENSITY (Arb. Units)
3.2
3.4
3.6
3.8
WAVELENGTH (μm)

Fig. 1

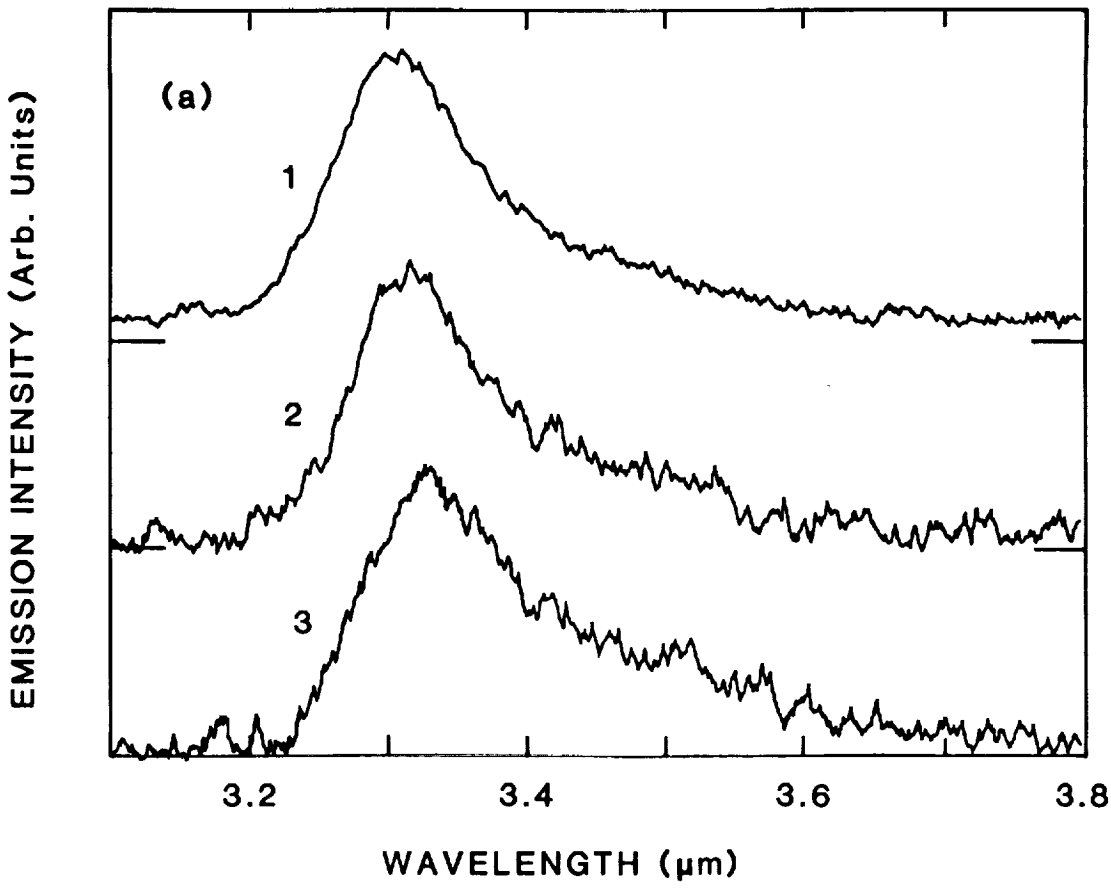
(a)
1
2
3
EMISSION INTENSITY (Arb. Units)
3.2
3.4
3.6
3.8
WAVELENGTH (μm)

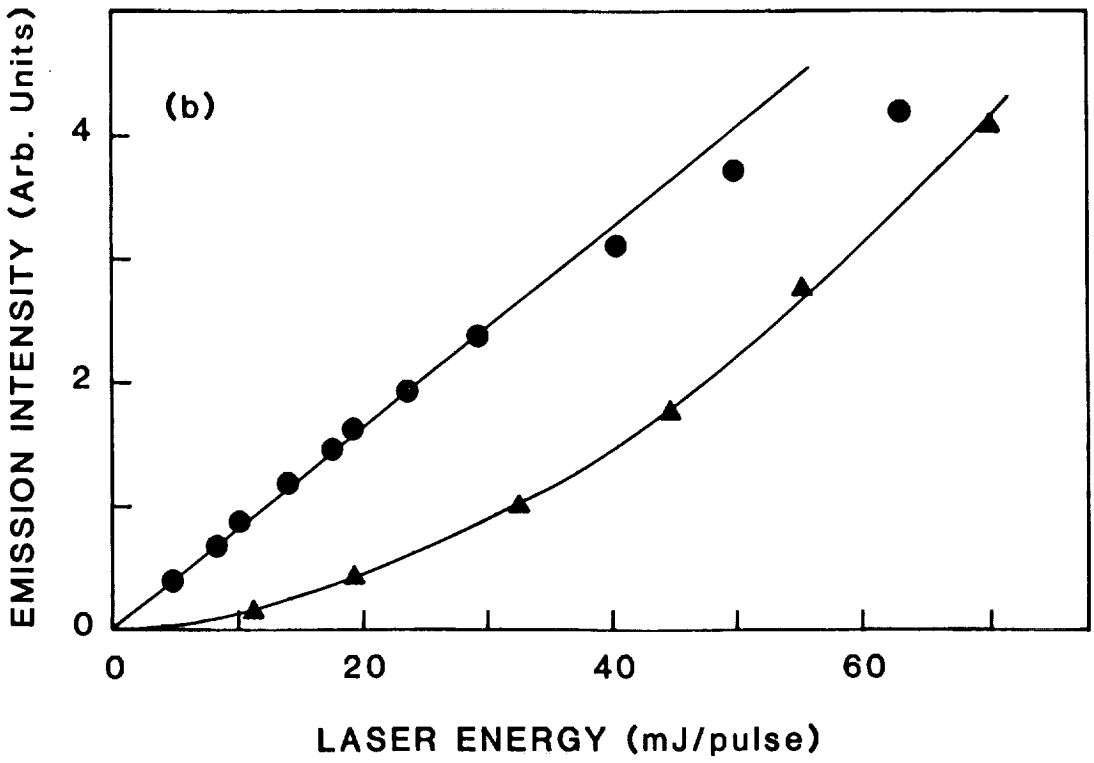
(b)
EMISSION INTENSITY (Arb. Units)
0
2
4
0
20
40
60
LASER ENERGY (mJ/pulse)

Fig. 2

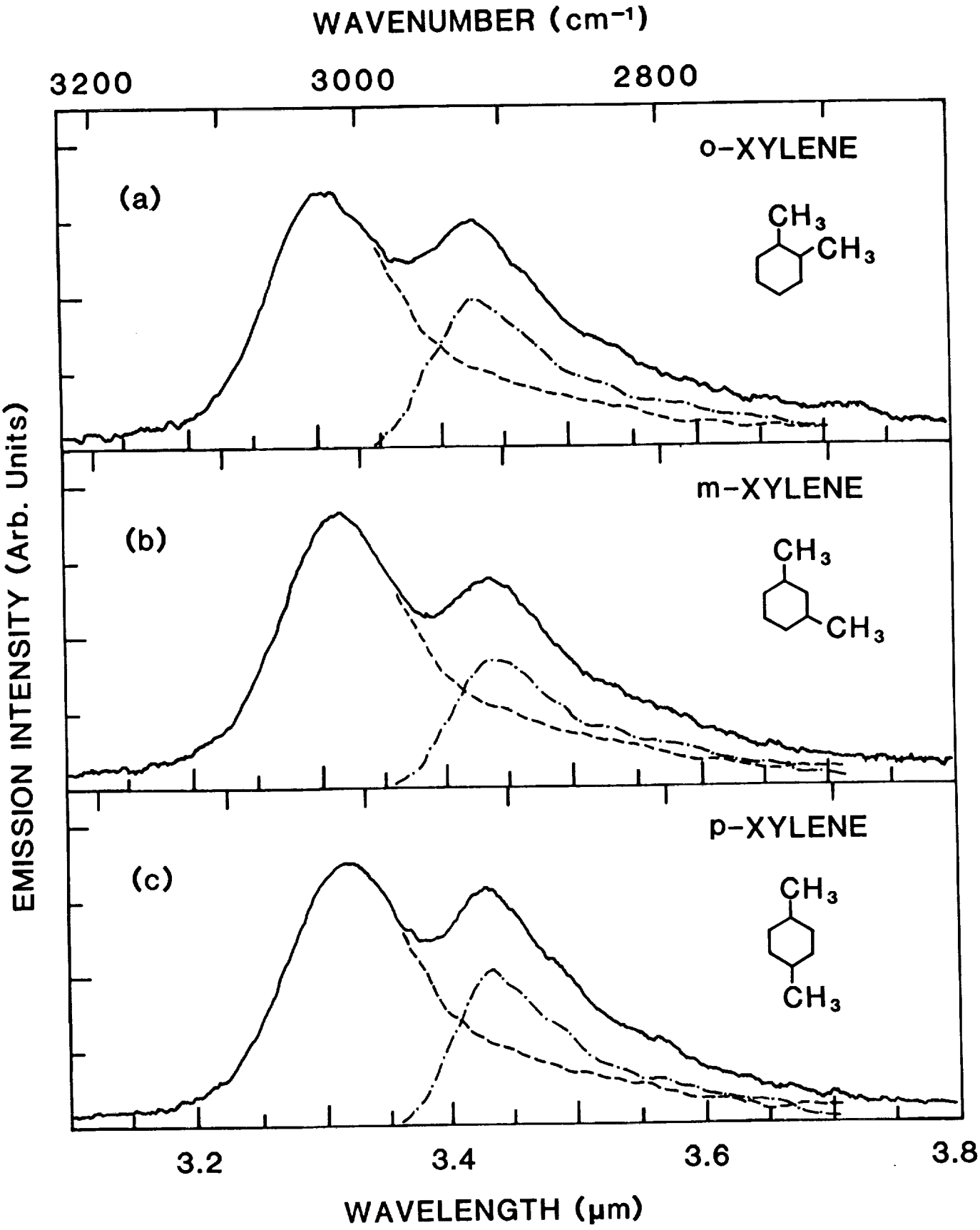
WAVENUMBER (cm⁻¹)
3200
3000
2800
o-XYLENE
(a)
CH3
CH3
m-XYLENE
(b)
CH3
CH3
p-XYLENE
(c)
CH3
CH3
EMISSION INTENSITY (Arb. Units)
3.2
3.4
3.6
3.8
WAVELENGTH (μm)

Fig. 3

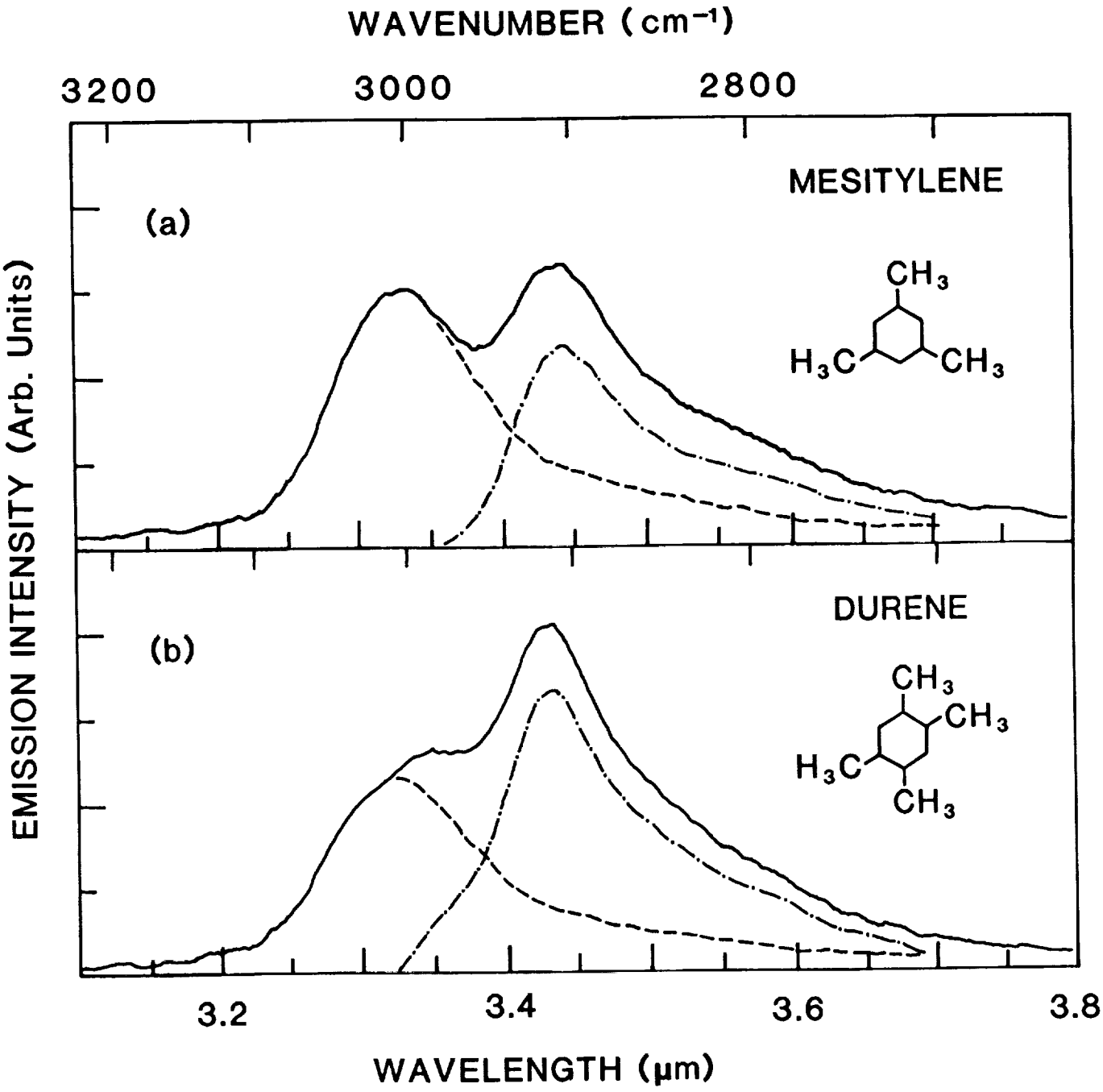
WAVENUMBER (cm⁻¹)
3200
3000
2800
MESITYLENE
(a)
CH3
H3C
CH3
DURENE
(b)
CH3
CH3
H3C
CH3
EMISSION INTENSITY (Arb. Units)
3.2
3.4
3.6
3.8
WAVELENGTH (μm)

Fig. 4

3.3 μm Emission from UV Excitation of Some Aromatic Molecules

Jun Shan, Masako Suto, and L. C. Lee

Molecular Engineering Laboratory

Department of Electrical and Computer Engineering

San Diego State University

San Diego, California 92182

Abstract

IR emissions are observed from photoexcitation of benzene, naphthalene, phenanthrene, anthracene, pyrene, and their methyl-derivatives in the gas phase at 193 nm using ArF laser as a light source. An emission band with peak at 3.3 μm is observed from all the molecules studied. This band is attributed to the aromatic C-H stretching vibrational modes. In addition to the 3.3 μm band, an emission band at 3.4-3.6 μm is observed from photoexcitation of the methyl-derivatives that is attributed to the C-H stretching vibrational modes of the CH_3 group. The observed spectra are compared with the IR emission bands observed in many astronomical objects. The current laboratory data lend a support to the model that PAH molecules are responsible for the "unidentified" interstellar IR emissions. IR emissions from the 193 nm excitation of several interstellar molecules other than PAHs are also observed that are quite different from the interstellar IR bands.

I. Introduction

Unidentified infrared (UIR) emission bands at 3.3, 6.2, 7.7, 8.6 and 11.3 μm have been observed in many astronomical objects, such as planetary nebulae, reflection rebulae, H II regions, and extragalactic sources (see reviews by Allanmandola 1984; Willner 1984; Allamandola et al. 1989). In addition to the main features, many objects show relative weak bands in the 3.4-3.6 μm region.

Several models have been proposed to identify the sources of the UIR bands. Duley and Williams (1981) proposed that the UIR bands might arise from some chemical functional groups (such as CH, CH_3, OH, CHO, and NH_2) chemisorbed on the surfaces of carbon particles. These functional groups give rise to IR spectral features characteristic of aromatic molecules. They suggested that the 3.3 and 11.3 μm emission bands are associated with resonances in aromatic C-H groups and the weak band at 3.4-3.6 μm is associated with aromatic methyl groups. Later, Allamandola, Tielens, and Barker (1985) and Léger and Puget (1984) proposed that the IR emissions were from the UV excitation of polycyclic aromatic hydrocarbons (PAH) of about 50 atoms. This UV pumping PAH model is supported by the good match between the UIR principal features and the absorption spectra of PAH molecules. The 3.3 μm band is uniquely assigned to the aromatic C-H stretching vibrational modes, but the assignment for the weak bands at 3.4-3.6 μm is subject to dispute. They are assigned to the overtones of the aromatic C-H stretching vibrational modes (Barker et al. 1987) or to the vibrational modes of the sidegroups (such as $-CH_3$, $-CH_2$, and -HCO) in the methyl-derivatives of PAH molecules (de Muizon et al. 1986).

Although the observations of the UIR bands are very extensive and the assignment of these bands to PAH molecules is very plausible, laboratory data

to support this claim are still lacking. IR emissions from the UV excitation of PAH molecules are critically needed to support the model. For this purpose, Cherchneff and Barker (1989) have recently observed the IR emission spectrum around 3.3 μm from photoexcitation of azulene ($C_{10}H_8$) at 308 nm. The IR emission from photoexcitation of benzene and its methyl derivatives at 193 nm has been recently observed in our laboratory (Shan et al. 1991), where both the 3.3 μm band and the satellite band at 3.4-3.6 μm are observed. The 3.4-3.6 μm band is correlated to the number of the CH_3 groups in the methyl-derivatives of an aromatic molecule. The IR observation is now extended to some PAH molecules in the gas phase, and the results are reported in this paper.

II. Experiment

The experimental setup was described in previous papers (Shan et al. 1991a,b). In brief, unfocused ArF excimer laser beam with a repetition rate of 10-20 Hz was used to excite molecules in a gas cell. Fresh sample gas was continuously introduced into the central region of a gas cell through a stainless steel tube of which the exit was near the laser path. For liquid samples, their vapor pressures at room temperature are high enough for experiments. For solids, the samples were heated up to obtain sufficient pressures for experiments. The tube that introduced the vapor to the gas cell was kept at a temperature higher than the temperature of sample container. The gas cell was continuously pumped by a mechanical pump with a dry-ice trap. In order to reduce carbon deposition on the entrance and exit windows along the laser path, the cell was extended with two 37-cm long arms, and the window regions were flushed by argon gas at about 1.6 Torr. The pressure in the chamber was monitored with a MKS Baratron manometer. The sample gas flow was

controlled by a needle valve so that the pressure at the exit of the tube was in equilibrium with the buffer gas. The laser intensity was limited to 50 mJ/pulse so that the emission intensity is linearly dependent on the laser power. The linear dependence ensures that our observation is not complicated by the multiphoton excitation process.

The IR emission observed through a CaF_2 window was dispersed by a 0.3-m monochromator (McPherson 218) in a direction perpendicular to the laser beam. A grating of 300 grooves/mm blazed at 3 μm was used for the dispersion. An aluminum-coated concave mirror was placed opposite to the monochromator entrance slit to enhance the emission collection efficiency. An infrared filter transmitting IR in the range of 2.2-4.1 μm (Corion RL-2000-F) was placed in front of the entrance slit to isolate the emission in the first-order region and also to eliminate the laser scattering light. The IR photons were detected by a 5-mm diameter InSb detector (Infrared Associates, Inc.) cooled by liquid N_2 (77 K). The signal from a matched preamplifier was accumulated by a boxcar integrator (EG&G) and processed by a microcomputer.

The spectral resolution used in the experiment was set at 0.025 μm. The spectral wavelength was calibrated by the 4th-6th order light of a He-Ne laser. The wavelength accuracy was estimated to be better than 0.005 μm. The spectral response for the detections system including window, filter, monochromator, and detector was calibrated against a black-body-spectral-radiance source (Infrared Industries) at 1250 K. The response of the detection system is shown in Fig.1(a) as the dashed line.

Liquid and solid chemicals were supplied by Aldrich Chemical Company with stated purities: benzene 99.9%, toluene 99%, o-xylene 98%, m-xylene 99% (with nitrogen protection), p-xylene 99%, mesitylene 99%, durene 98%, naphthalene 99%, 1-methylnaphalene 98%, 2-methylnaphlalene 98%, anthracene 99.9%,

9-methylanthracene 98%, phenanthrene 98%, pyrene 99%, heptane 99.9%, acetone 99.9%, methanol 99.9% and cycopentane (with saturated C_5 hydrocarbons) 99%. The dimethylnaphthalene was a mixture of isomers supplied by Aldrich. Allene (97.0%), ethylene (99.5%), and 1,3-butadiene (99.0%) were from Matheson Gas Products. Ethylacetylene (95.0%), trans-2-butene (99.0%), and 3-methyl-1-butene (CP Grade) were from Union Carbide Corporation. All liquid and solid chemicals were degassed before using for experiments.

III. Results

A. Benzene and Methyl-Derivatives

The IR emissions at 3.1-3.8 μm from photoexcitation of benzene and its methyl-derivatives (toluene, xylenes, mesitylene and durene) have been reported in a previous paper (Shan et al 1990). Here, we only give a summary. Fig.1(a) shows the IR spectrum of benzene excited by 193 nm photons at pressures about 1.6 Torr. (In the current experimental setup, the sample concentration in the laser irradiation region is difficult to determine accurately, but it may be nearly equal to the equilibrium pressure). The emission band with a peak at 3.3 μm corresponds to the $v = 1 \rightarrow 0$ transition of the C-H stretching vibrational modes. The FWHM of the band is 0.12 ± 0.01 μm. The intensity for the $v = 2 \rightarrow 1$ transition of the C-H stretching modes at 3.42 μm (2925 cm^{-1}) (Reddy et al. 1982) is much weaker than the $v = 1 \rightarrow 0$ transition.

In addition to the 3.3 μm band, an emission band with peak around 3.43 μm is observed from photoexcitation of toluene, p-xylene, mesitylene and durene as shown in Figs.1(b,c,d, and e). The intensity of the 3.43 μm band increases with the number of the CH_3 groups in the benzene derivatives, indicating that this band is associated with the CH_3 group. The bandwidth of the 3.3 μm

emission is about 0.12 μm, which is much broader than those observed in the UIR bands that are in the range 0.02-0.05 μm. Since the FWHM of an IR emission band may depend on the molecular size, it is of interest to investigate other PAH molecules. Large PAH molecules are more stable under the interstellar UV field, so they are more likely responsible for the UIR emissions (Allamandola et al. 1989; Puget and Léger 1989).

B. PAH Molecules

The IR emissions from photoexcitation of naphthalene and its methyl derivatives (1-methylaphthalene, 2-methylaphthalene and dimethylnaphthalene) at 193 nm are shown in Fig.2. The samples were heated to 70-90°C to obtain sufficient vapor pressures for experiments. The 3.3 μm band observed from naphthalene has a bandwidth ~ 0.085 μm that is much narrower than that of benzene, but it is still wider than the UIR band. The bandwidths of the molecules measured under the same apparatus at a spectral resolution of 0.025 μm are listed in Table 1. The spectral profile of naphthalene in Fig.2(a) is asymmetrical, but the intensity of the $v = 2 \rightarrow 1$ transition at 3.4 μm is quite small.

The IR emission spectra observed from the methyl-derivatives of naphthalene are shown in Figs.2 (b,c and d), where an additional band is shown in the 3.4-3.6 μm region. The spectra shown in Fig.2 are very similar to those observed from benzene and its derivatives. These results further support that the 3.4-3.6 μm band associates with the CH_3 group.

Figs.3 (a, b, c, and d) show the IR emission spectra observed from photoexcitation of phenanthrene, anthracene, 9-methylanthracene, and pyrene at 193 nm, respectively. In order to obtain sufficient vapor pressures for experiments, the samples were heated at 140-180°C. The peaks of the emission

signals are normalized to the same magnitude, where the signal level is larger, if the noise level is lower. The signal intensity depends on laser power and gas concentration. The 3.3 μm band shows up in every spectrum, and the spectral profiles of phenanthrene, anthracene, and pyrene are all similar to that of naphthalene, except for the peaks being slightly shifted as shown in Table 1. The FWHMs of the spectra are all about 0.085 μm. The spectrum from photoexcitation of 9-methylanthracene shows a peak at 3.40 μm as shown in Fig.3(c). Again, this band is attributable to the C-H stretching vibrational modes of the CH_3 group. The wavelength of the peak at 3.40 μm is shorter than those of the methyl-derivatives of benzene and naphthalene at 3.43 μm.

PAHs at room temperature are in solids which are heated up to obtain sufficient vapor pressures for experiments. The impurities of small molecular sizes will be evaporated at relative low temperatures before the true sample is evaporated. In our experiment, the sample was continuously heated up, and the emission spectra were repeatedly observed until the sample in the container was substantially evaporated. It is believed that the spectra shown in Figs.2 and 3 are genuinely produced by the molecules specified.

All the aromatic molecules studied emit the 3.3 μm band, and their methyl-derivatives emit the additional band at 3.4-3.6 μm. It is of interest to examine whether other interstellar molecules can emit these bands. Thus, the IR emissions from other molecules were observed for comparison.

C. Other Interstellar Molecules

IR emissions from photoexcitation of interstellar molecules other than aromatic molecules were searched in the 3-4 μm region. The emissions from H_2O, H_2CO, CH_3OH, ethylene (C_2H_4), allene (C_3H_4), ethylacetylene (C_2H_5CCH), heptane ($CH_3(CH_2)_5CH_3$) and cyclopentane (C_5H_{10}) are too weak to disperse, when

they are excited by the 193 nm photons at pressures about 2 Torr.

IR emissions are observed from the 193 nm photoexcitation of acetone, trans-2-butene, 1,3-butadiene, and 3-methyl-1-butene, for which the emission spectra at vapor pressures about 2 Torr are shown in Fig. 4. The IR emission in the 2.9-4.0 μm region was observed from photoexcitation of acetone at 193 nm by Donaldson and Leone (1986). The emission at the wavelengths shorter than 3.2 μm is not detected in the current experiment because of small detection response. The emission is attributed to the CH_3 free radial in the gas phase. The spectra shown in Fig.4 are quite different from those of aromatic molecules and the UIR bands. The bandwidths are very broad, and their wavelengths vary with molecules. These results show that the emissions from these molecules are not related to the UIR bands, although they may contribute to the IR bands observed in some astronomical objects.

IV. Comparison with the UIR Bands

The 3.3 μm emission band has been observed in many astronomical objects such as planetary nebulae, bipolar nebulae, H II region, stars, IRAS sources, Orion bar region, etc. (Allen et al. 1982; Gillett et al. 1973; de Muizon et al. 1986, 1990 a,b; Geballe et al 1985, 1989 a,b; Nagata et al. 1988; Russell et al. 1977; Sellgren, 1984; Sellgren et al. 1990; Tokunaga et al. 1988). The weak emission at 3.4-3.6 μm generally accompanies with the 3.3 μm band, but the intensity ratios of these two bands vary with objects. The broad band is resolved into weak structures at 3.40, 3.46, 3.51, and 3.56 μm (de Muizon et al. 1986, 1990b).

The current emission spectra are remarkably similar to the 3.3 μm UIR band. For example, the UIR spectra observed from (a) the IRAS 21282 + 5050 (de Muizon et al. 1986), (b) the Orion position 4 (Sellgren et al. 1990), and

(c) the H II region S106 (Geballe et al. 1985) are selected to compare with the spectrum of 9-methylanthracene as shown in Fig.5. We deliverily select the UIR spectra that have spectral resolutions similar to the current experiment so that they can be closely compared. The band peaks at 3.29 and 3.40 μm are about the same for all spectra shown in Fig.5, but the current bandwidth of the 3.3 μm band is broader than those of the UIR bands. The difference is subject to discussion below. It is worth noting that the 3.3 μm UIR band is quite different from the emission spectra of other interstellar molecules shown in Fig.4.

V. Discussion

The possible sources for the UIR emissions have been extensively investigated (Allamandolla et al. 1985, 1987, 1989; Barker et al. 1987; Borghesi 1987; Desert et al. 1986, 1990; Duley and Williams 1981; Geballe et al. 1989b; Léger and d'Hendecourt 1987; Léger and Puget 1984; Léger et al. 1989; Puget and Léger 1989). Now it is generally consented that the UIR emissions are mainly produced by the UV excitation of large PAH molecules. The current laboratory data support this model as demonstrated by the remarkably similar spectra shown in Fig. 5. However, the good match is only circumstantial. In the interstellar medium, the PAH-related species are enormous that include neutral, ionized, and radical forms; each species is well isolated; and the interstellar UV light is wide spanned over the 91-250 nm region. In contrast, we study only a single chemical species at a time; the excited molecules are subject to quenching; and the excitation photon wavelength is around 193 nm. It is not feasible to observe the IR emissions in a laboratory same as the interstellar conditions. Because of different conditions, the emission spectra are expected to show differences in some

aspects. Nevertheless, it may not be a coincidence that the UIR spectra are in good match with those of PAH molecules but not other classes of interstellar molecules. Thus, the current laboratory data do lend a support to the model that PAH molecules are responsible for the UIR emissions.

There is no dispute that the UIR 3.3 μm band is associated with the aromatic C-H stretching vibrational modes. However, the overtones of the aromatic C-H stretching vibrational modes do not show distinct emission intensity in the 3.4-3.6 μm region; thus, they are not responsible for the UIR emission. Instead, the 3.4-3.6 μm bands are commonly observed from photoexcitation of the methyl-derivatives of aromatic molecules; thus, the UIR 3.4-3.6 bands are likely associated with the CH_3 group.

IR emission bands with peaks at 3.43 and 3.53 μm bands are shown in the spectra observed toward the objects, HD97048, Elias 1, and HR4049 (Aitken and Roche 1981; Allen et al. 1982; Baas et al. 1983; Blades and Whittet 1980; Schutte et al. 1990; Van der Zwet 1985; Whittet et al. 1983). These bands are quite different from the 3.40-3.60 μm band observed in the current spectra, thus, they are not associated with the CH_3 groups in the methyl-derivatives of aromatic molecules.

VI. Concluding Remarks

The IR emissions in the 3.2-3.8 μm region are observed from photoexcitation of several aromatic molecules in the gas phase at 193 nm. A 3.3 μm emission band is commonly observed from all the molecules studied, and an additional band is observed at 3.4 -3.6 μm from the methyl-derivatives of aromatic molecules. The current results lend a support to the model that the UIR emission bands observed in many astronomical objects are produced by the UV excitation of PAH molecules. The UIR 3.3 μm is likely associated with the

aromatic C-H stretching vibrational modes, and the 3.4-3.6 μm band is associated with the CH_3 groups of the methyl-derivatives of aromatic molecules. The IR emissions from photoexcitation of several interstellar molecules other than the aromatic molecules are observed, but they are quite different from the UIR bands; thus, they are not responsible for the UIR bands.

Acknowledgement

This paper is based on the work support by the NASA under Grant No. NAGW-319.

References

Aitken, D. K. and Roche, P. F. 1981, M. N. R. A. S., **196**, 39P.

Allamandola, L. J. 1984, in **Galactic and Extragalactic Infrared Spectroscopy**, ed. M. F. Kessler and J. P. Philips, (Dordrecht; Reidel), p.5.

Allamandola, L. J., Sandford, S. A., and Wopenka, B. 1987, Science, **237**, 56.

Allamandola, L. J., Tielens, A. G. G. M., and Barker, J. R. 1985, Ap. J. Lett., **290**, L25.

Allamandola, L. J., Tielens, A. G. G. M., and Barker, J. R. 1989, Ap. J. Suppl. Ser., **71**, 733.

Allen, D. A., Baines, D. W. T., Blades, J. C., and Whittet, D. C. B. 1982, M. N. R. A. S., **199**, 1017.

Baas, F., Allamandola, L. J., Geballe, T. R., Persson, S. E., and Lacy, J. H. 1983, Ap. J., **265**, 290.

Barker, J. R., Allamandola, L. J., and Tielens, A. G. G. M. 1987, Ap. J. (Letters), **315**, L61.

Blades, J. C. and Whittet, D. C. B. 1980, M. N. R. A S., **191**, 701.

Borghesi, A., Bussoletti, E., and Colangeli, L. 1987, Ap. J. **314**, 422.

Cherchneff, I. and Barker, J. R. 1989, Ap. J. (Letters), **341**, L21.

de Muizon, M., Geballe, T. R., d'Hendecourt, L. B., and Baas, F. 1986, Ap J. (Letters), **306**, L105.

de Muizon, M. J., d'Hendecourt, L. B., and Geballe, T. R. 1990a, Astron. Astrophys. **227**, 526.

de Muizon, M. J., d'Hendecourt, L. B., and Geballe, T. R. 1990b, Astron. Astrophys. **235**, 367.

Desert, F. X., Boulanger, F., Léger, A., Puget, J. L., and Sellgren, K. 1986, Astron. Astrophys. **159**, 328.

Desert, F. X., Boulanger, F., and Puget, J. L. 1990 Astron. Astrophys. **237**, 215.

Donaldson, D. J. and Leone, S. R. 1986, J. Chem. Phys., **85**, 817.

Duley, W. W. and Williams, D. A. 1981, M. N. R. A. S.,**196**, 269.

Geballe, T. R., Lacy, J. H., Persson, S. E., McGregor, P. J., and Soifer, B. T. 1985, Ap. J., **292**, 500.

Geballe, T. R., Noll, K. S., Whittet, D. C. B., and Waters, L. B. F. M. 1989a, Ap. J. (Letters) **340**, L29.

Geballe, T. R., Tielens, A. G. G. M., Allamandola, L. J., Moorhouse, A., and Brand, P. W. J. L. 1989b, Ap. J. **341**, 278.

Gillett, F. C., Forrest, W. J. and Merrill, K. M. 1973, Ap. J., **183**, 87.

Léger, A. and d'Hendecourt, in **Polycyclic Aromatic Hydrocarbons and Astrophysics**, ed. Léger, A., d'Hendecourt, L., and Boccara, N. 1987, D. Reidel Publishing, Dordrecht, p.223.

Léger, A., d'Hendecourt, L., and Défourneau, D. 1989, Astron. Astrophys. **216**, 148.

Léger, A. and Puget, J. L. 1984, Astron. Astrophys. **137**, L5.

Nagata, T., Tokunaga, A. T., Sellgren, K., Smith, R. G., Onaka, T., Nakada, Y., and Sakata, A. 1988, Ap. J., **326**, 157.

Puget, J. L. and Léger, A. 1989, Annu. Rev. Astron. Astrophys. **27**, 161.

Reddy, K. V., Heller, D. F., and Berry, M. J. 1982, J. Chem. Phys., **76**, 2814.

Russell, R. W., Soifer, B. T., and Merrill, K. M. 1977, Ap. J., **213**, 66.

Schutte, W. A., Tielens, A. G. G. M., Allamandola, L. J., Cohen, M., and Wooden, D. H. 1990, Ap. J., **360**, 577.

Sellgren, K. 1984, Ap. J., **277**, 623.

Sellgren, K., Tokunaga, A. T., and Nakada, Y. 1990, Ap. J. **349**, 120.

Shan, J., Suto, M., and Lee, L. C. 1991, submitted to Chem. Phys. Lett. for Publication.

Shan, J., Suto, M., and Lee, L. C. 1991b, J. Quant. Spectrosc. Radiat. Transfer **45**, 139.

Tokunaga, A. T., Nagata, T., Sellgren, K., Smith, R. G., Onaka, T., Nakada, Y., Sakata A., and Wada, S. 1988, Ap. J. **328**, 709.

van der Zwet, G. P., Allamandola, L. J., Baas, F., and Greenberg, J. M. 1985, Astron. Astrophys., **145**, 262.

Whittet, D. C. B., Williams, P. M., Bode, M. F., Davies, J. K., and Zealey, W. J. 1983, Astron. Astrophys., **123**, 301.

Willner, S. P. 1984 in Galactic and Extragalactic Infrared Spectroscopy, ed. M. F. Kessler, and J. P. Philips, (Dordrecht: Reidel), p.37.

Table I The bandwidths of the 3.3 μm emission from photoexcitation of aromatic molecules at 193 nm.

Molecule	Peak (μm)	FWHM (μm)
Benzene	3.30	0.12
Naphthalene	3.29	0.085
Phenanthrene	3.30	0.085
Anthracene	3.30	0.086
Pyrene	3.31	0.082

Figure Captions

Fig.1 IR emission spectra observed from the 193 nm excitation of (a) benzene, (b) toluene, (c) p-xylene, (d) mesitylene, and (e) durene. The spectral resolution for the spectra was set at 0.025 μm. The dashed line in (a) is the response of the detection system.

Fig.2 IR emission spectra observed from the 193 nm excitation of (a) naphthalene, (b) 1-methylnaphthalene, (c) 2-methylnaphthalene, and (d) dimethylnaphthalene.

Fig.3 IR emission spectra observed from the 193 nm photoexcitation of (a) phenanthrene, (b) anthracene, (c) 9-methylanthracene, and (d) pyrene.

Fig.4 IR emission spectra observed from the 193 nm excitation of (a) acetone, (b) trans-2-butene, (c) 1,3-butadiene, and (d) 3-methyl-1-butene.

Fig.5 Comparison of the UIR spectra observed from (a) IRAS, (b) Orion, and (c) H II region with that of (d) 9-methylanthracene. The spectral resolutions in μm are (a) 0.033, (b) 0.019, (c) 0.095, and (d) 0.025.

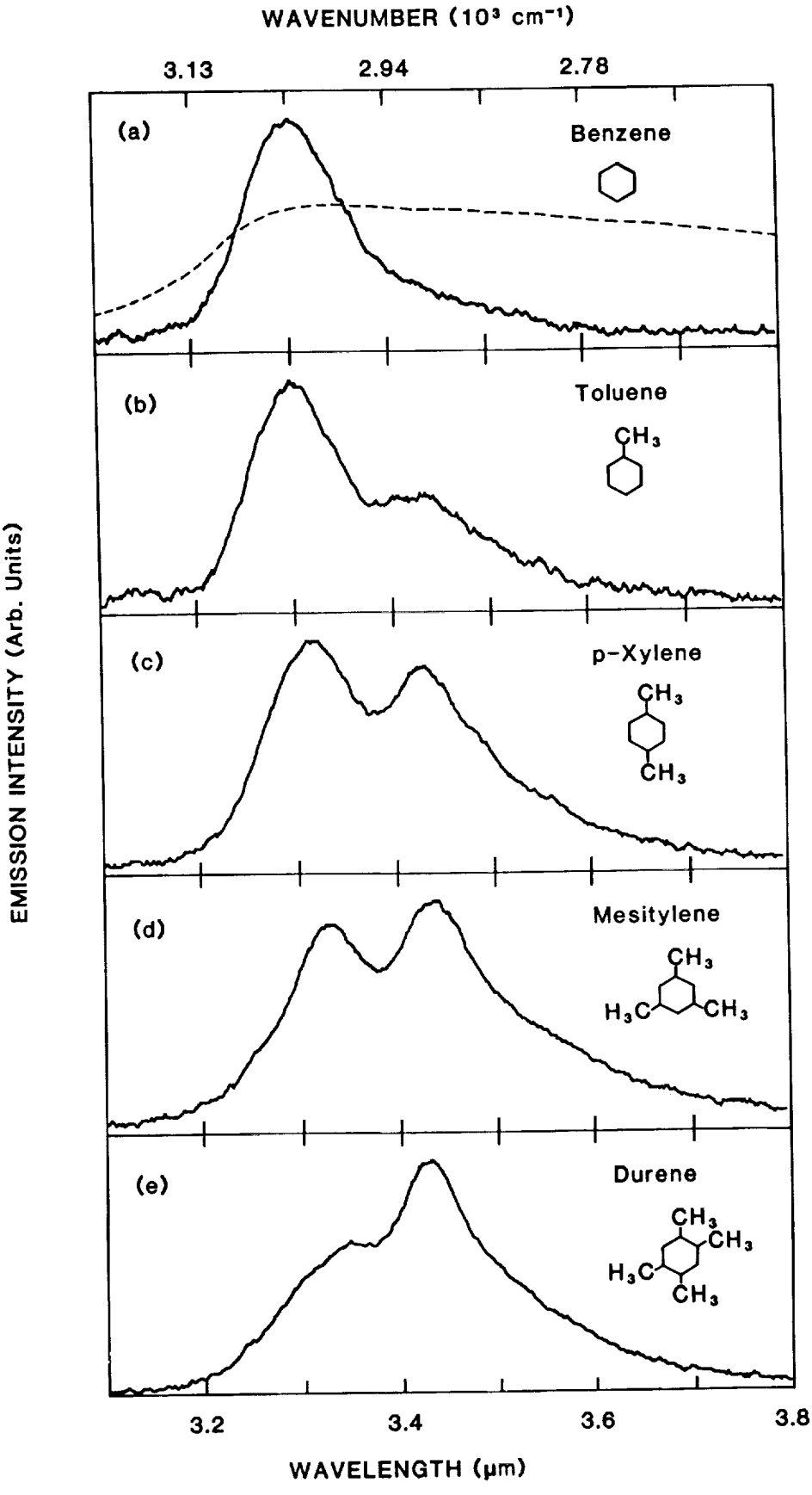
WAVENUMBER (10^3 cm^{-1})
3.13
2.94
2.78
(a)
Benzene
(b)
Toluene
CH_3
(c)
p-Xylene
CH_3
CH_3
(d)
Mesitylene
CH_3
H_3C
CH_3
(e)
Durene
CH_3
CH_3
H_3C
CH_3
EMISSION INTENSITY (Arb. Units)
3.2
3.4
3.6
3.8
WAVELENGTH (μm)

Fig. 1

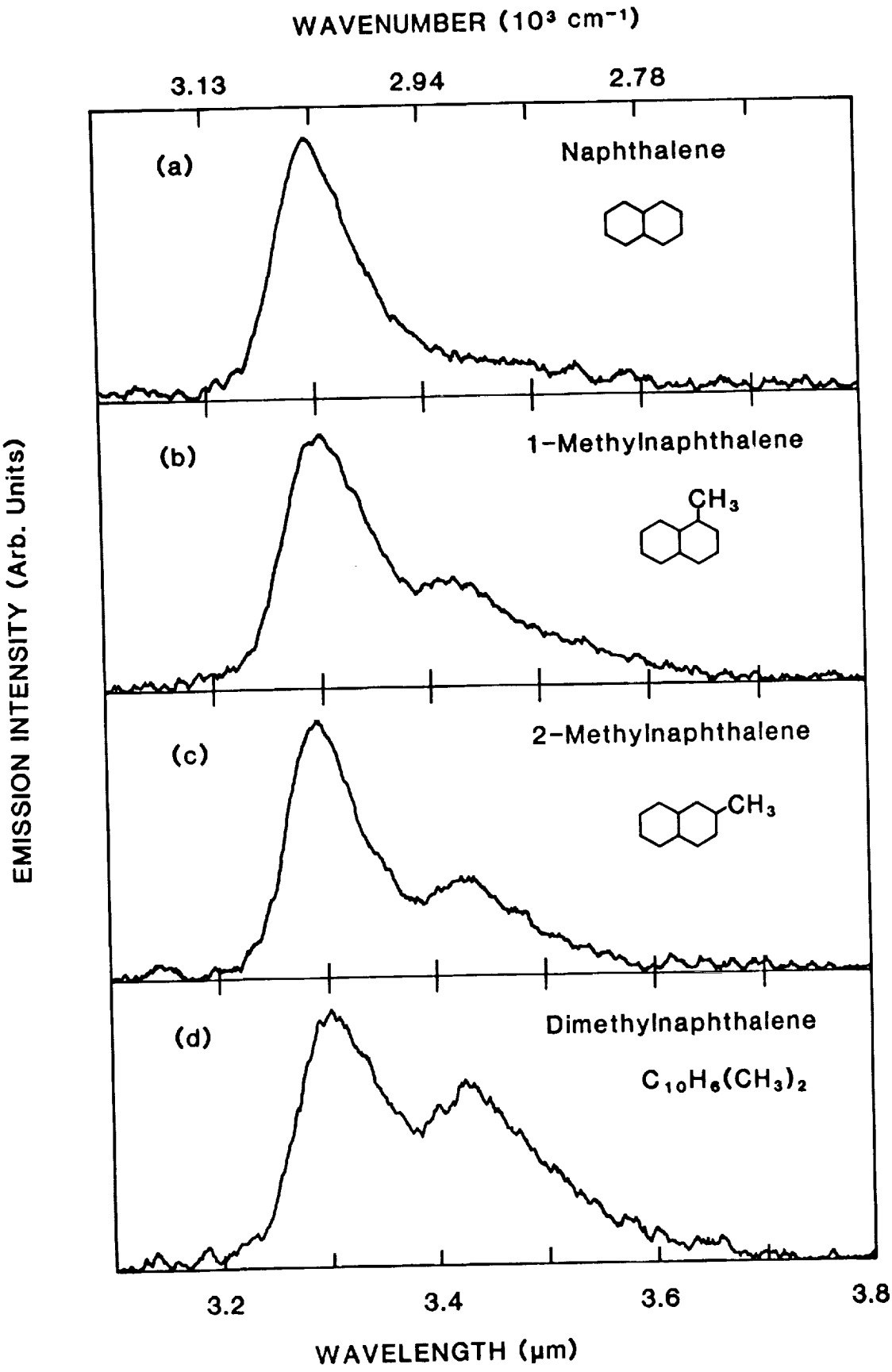
WAVENUMBER (10^3 cm^{-1})
3.13
2.94
2.78
(a)
Naphthalene
(b)
1-Methylnaphthalene
CH_3
(c)
2-Methylnaphthalene
CH_3
(d)
Dimethylnaphthalene
$C_{10}H_6(CH_3)_2$
EMISSION INTENSITY (Arb. Units)
3.2
3.4
3.6
3.8
WAVELENGTH (μm)

Fig. 2

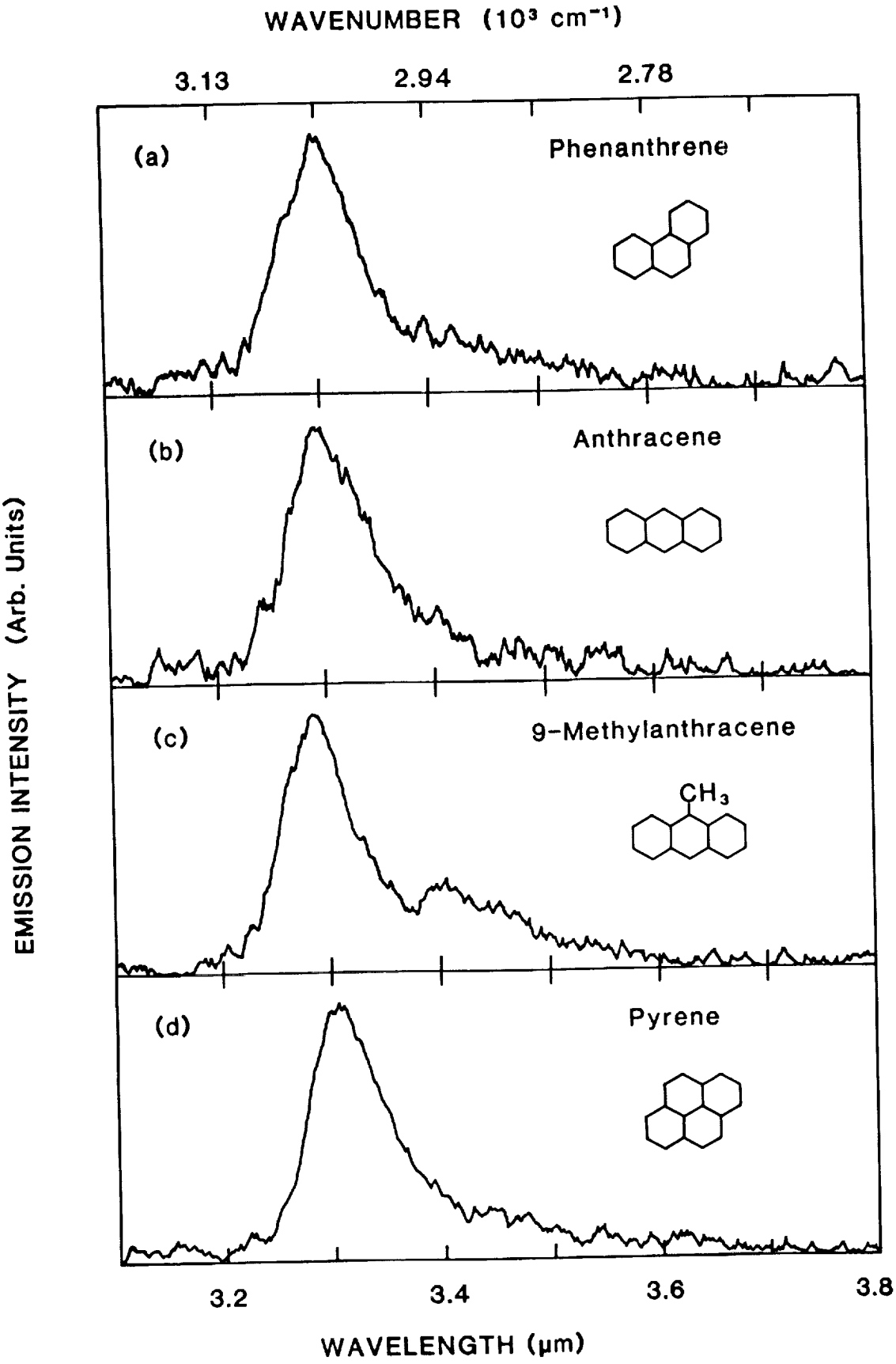
WAVENUMBER (10³ cm⁻¹)
3.13
2.94
2.78
(a)
Phenanthrene
(b)
Anthracene
(c)
9-Methylanthracene
CH₃
(d)
Pyrene
EMISSION INTENSITY (Arb. Units)
3.2
3.4
3.6
3.8
WAVELENGTH (μm)

Fig. 3

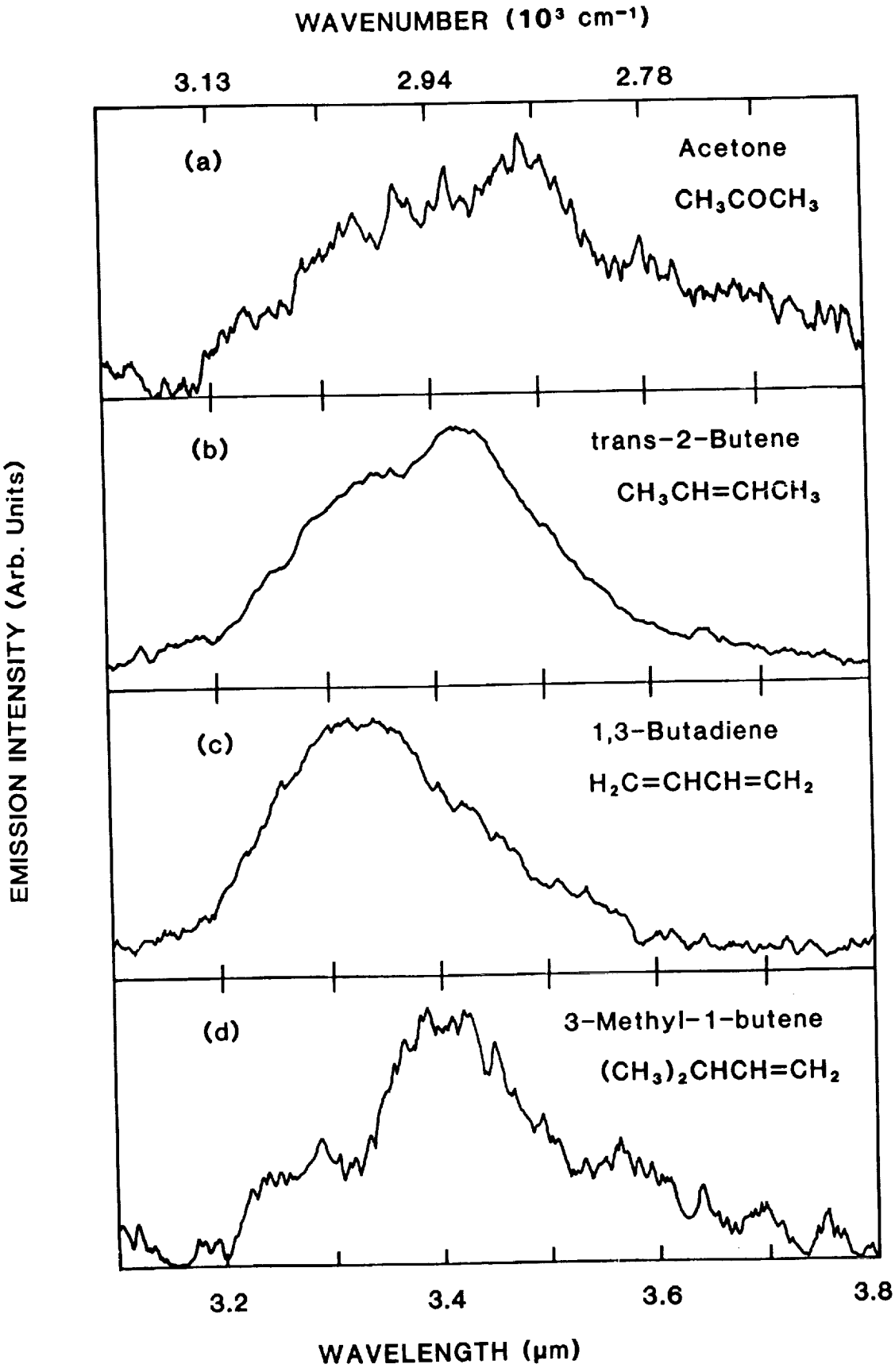

Fig. 4

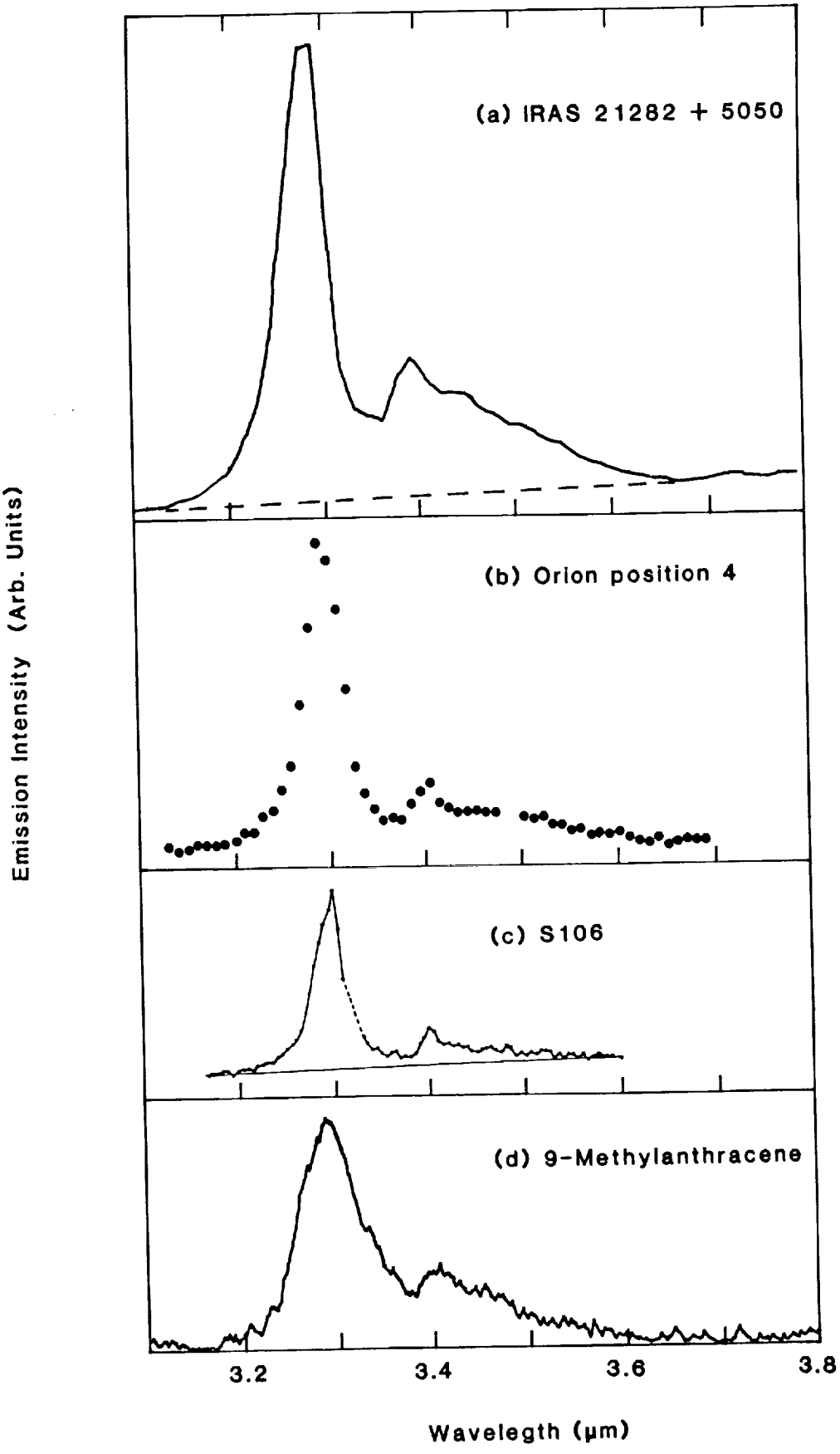
(a) IRAS 21282 + 5050
(b) Orion position 4
(c) S106
(d) 9-Methylanthracene
Emission Intensity (Arb. Units)
3.2
3.4
3.6
3.8
Wavelegth (μm)

Fig. 5

J. Quant. Spectrosc. Radiat. Transfer Vol. 44, No. 4, pp. 379–391, 1990
Printed in Great Britain.

0022-4073/90 $3.00 + 0.00

FLUORESCENCE FROM EXCITATION OF CH_4, CH_3OH AND CH_3SH BY EXTREME VACUUM ULTRAVIOLET RADIATION

GUANG MA, MASAKO SUTO, and L. C. LEE†
Molecular Engineering Laboratory, Department of Electrical and Computer Engineering, San Diego State University, San Diego, CA 92182, U.S.A.

(*Received* 22 *March* 1990)

Abstract—The photoabsorption and fluorescence cross sections of CH_4, CH_3OH, and CH_3SH were measured in the wavelength regions of 52–106, 48–106, and 48–106 nm, respectively. The fluorescence spectra were dispersed to identify the emitting species. Emissions from the excited species of H* and CH* are commonly observed for all three molecules. Emission from the excited CH_2^* is observed from CH_4, OH* from CH_3OH, and CS* from CH_3SH. The photoexcitation processes that may produce the observed emission bands are discussed.

INTRODUCTION

Fluorescence from excitation of molecules by vacuum ultraviolet (vuv) radiation has received continuous study in our laboratory; and the results obtained from CH_4, CH_3OH, and CH_3SH are reported in this paper. The absorption cross sections have been measured extensively for CH_4, moderately for CH_3OH, but very little for CH_3SH. Fluorescence from vuv excitation of CH_4 has been observed.[1–5] An excitation band that produces the u.v.-visible fluorescence has been observed[1] in the 75–103 nm region. The fluorescence was dispersed[2] and the emission systems were identified to be $CH(A^2\Delta, B^2\Sigma \rightarrow X^2\Pi)$, $H(n \geqslant 3 \rightarrow n = 2)$ and $CH_2(\tilde{b}\ ^1B_1 \rightarrow \tilde{a}\ ^1A_1)$. The fluorescence cross section in the $\lambda > 106$ nm region measured in an earlier experiment[2] was much smaller than the later data.[5] At $\lambda < 106$ nm, the earlier values[2] are also much smaller than the current measurement. This difference arouses interest for reinvestigation of CH_4 fluorescence.

In contrast to CH_4, the fluorescence from vuv excitation of CH_3OH has not been studied extensively. $OH(A\ ^2\Sigma^+ \rightarrow X\ ^2\Pi_i)$ emission has been observed in the excitation wavelength region of $\lambda > 87$ nm,[6,7] but the emissions from the excited species H* and CH* have not been reported previously. For CH_3SH, only CH_3S^* emission is reported in the 130–175 nm region.[8] H* and CH* emissions were expected from photoexcitation of this molecule and were observed in the current experiments. An unexpected $CS(A\ ^1\Pi \rightarrow X\ ^1\Sigma^+)$ emission was also observed from this molecule.

The fluorescence data are useful for investigation of molecular photodissociation processes. Quantitative vuv spectroscopic data are needed for the study of interstellar photochemistry, because CH_4, CH_3OH, and CH_3SH molecules exist in the interstellar medium.

EXPERIMENTAL

The photoabsorption and fluorescence cross sections were measured using synchrotron radiation produced by the electron storage ring at the University of Wisconsin. The experimental setup has been described in previous papers.[9,10] Thin-film windows of Al, Sn, and In were used for measurements in the regions of 48–60, 54–76, and 74–106 nm, respectively. These windows were used to separate the high-vacuum monochromator from the gas cell (3.5 cm dia and 40.9 cm long), as well as to cut off high-order light. The sample gas was slowly pumped by a sorption pump. The fluorescence was observed simultaneously with the absorption measurement in a direction perpendicular to the light path.

†To whom all correspondence should be addressed.

The apparatus used for the fluorescence-dispersion experiment has been depicted in a previous paper.[10] In brief, the light source was a condensed-capillary discharge lamp that was discharged by a 10 kV d.c. power supply pulsed by a hydrogen thyratron. The discharge medium was Ar or N_2 with a trace of O_2. The atomic ion emission lines in the 45–200 nm region were selected by a 1-m vacuum monochromator. There were no windows in the light path. The fluorescence was dispersed by an optical multichannel analyzer with variable time delay and gate duration.

CH_4 was supplied by Matheson with a stated purity better than 99.99%. CH_3SH was supplied by Matheson and Aldrich with stated purities better than 99.5%. The CH_3OH vapor was obtained from methanol liquid supplied by Fisher Scientific with a stated purity better than 99.9%.

RESULTS

CH_4

The absorption and fluorescence cross sections of CH_4 in the 52–106 nm region are shown in Figs. 1(a) and (b), respectively. The quantum yield, which is determined by the ratio of fluorescence to absorption cross sections, is shown in Fig. 1(c). In our measurements, the uncertainty is generally estimated to be $\pm 10\%$ for the absorption cross section and $\pm 30\%$ for the fluorescence cross section. The weak absorption structure reported in the previous paper[3] is omitted in Fig. 1(a). The absorption cross section is systematically smaller than the value recommended by Berkowitz,[11] but it agrees excellently with the data of Samson and Haddad.[12] The fluorescence cross section in the 52–62 nm region was reported in a previous paper[3] and is replotted in Fig. 1(b), for which the maximum cross section is 1.6×10^{-20} cm^2 at 56 nm. Since the fluorescence quantum yield is so small ($< 1.6\%$), the experimental uncertainty is high.

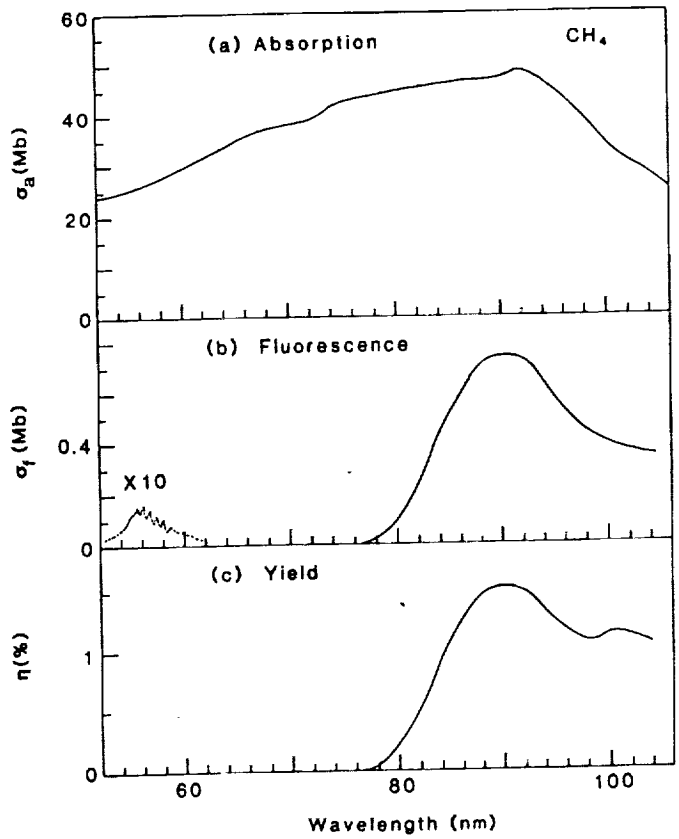

Fig. 1. Absorption cross section (a), fluorescence cross section (b), and fluorescence quantum yield (c) of CH_4 in the 52–106 nm region. The cross section is in units of Mb (10^{-18} cm^2), and the quantum yield is in percent.

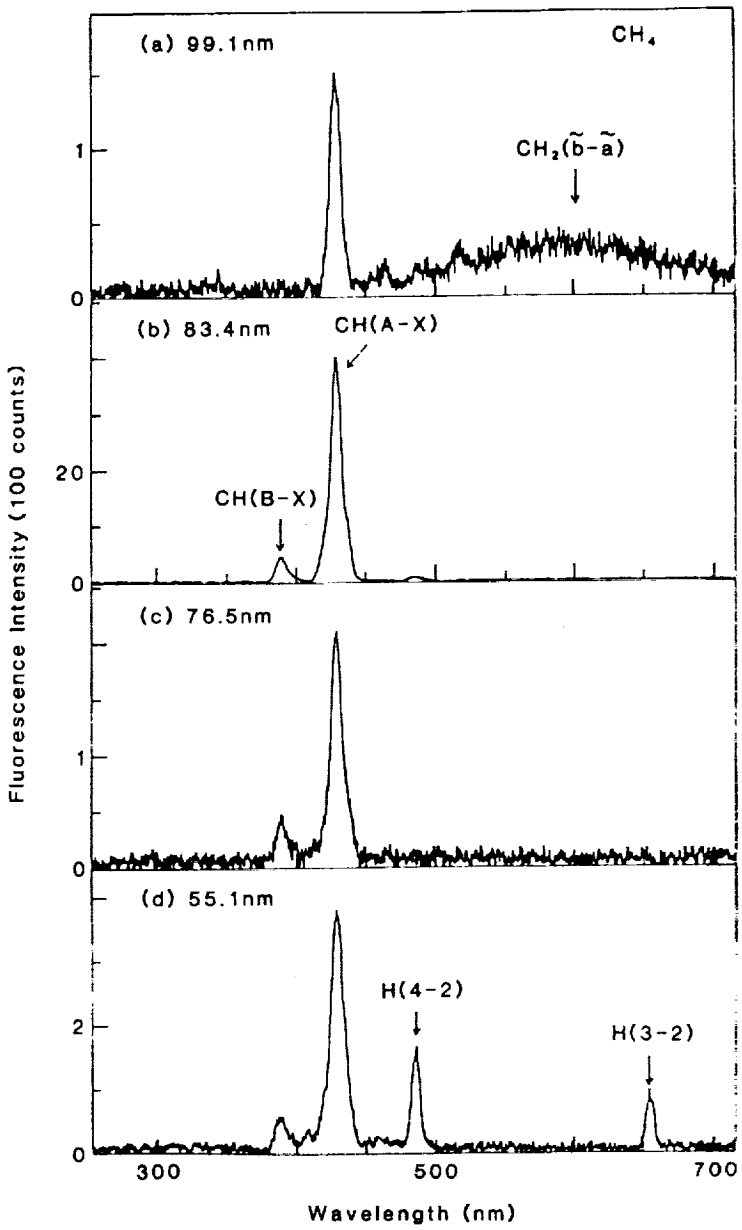

Fig. 2. Fluorescence spectra produced by photoexcitation of CH_4 at the excitation wavelengths of 99.1–55.1 nm. The identifications for the emission bands are indicated.

The fluorescence cross sections in the 80–106 nm region are generally larger than the previous data[2] by about one order of magnitude. The value of about 3.7×10^{-19} cm^2 at 106 nm is, however, consistent with the later measurement.[5] The earlier data[2] were measured at gas pressures of ~ 150 mtorr, which are much higher than those employed in the current experiments. Because of the high gas pressures used, the earlier data may be distorted by preabsorption and quenching effects that were not considered in the experiments.[2]

Fluorescence spectra from photoexcitation of CH_4 were observed at several excitation wavelengths in the 45.6–103.7 nm region. The spectra observed at 99.1, 83.4, 76.5, and 55.1 nm are shown in Figs. 2(a)–(d), respectively. The fluorescence consists of the CH($A, B \rightarrow X$), $CH_2(\tilde{b} \rightarrow \tilde{a})$, and H($n - 2$) systems. The CH($A \rightarrow X$) and CH($B \rightarrow X$) systems start to appear at 99.1 and 95.5 nm, respectively, and they become stronger at the shorter excitation wavelengths. The $CH_2(\tilde{b} \rightarrow \tilde{a})$ system starts at 132 nm and reaches a peak at about 106 nm.[4] The emission becomes very weak at 87.8 nm. In Fig. 3, the spectra at 99.1, 95.5, 92.3, and 87.8 nm are amplified to show the weak

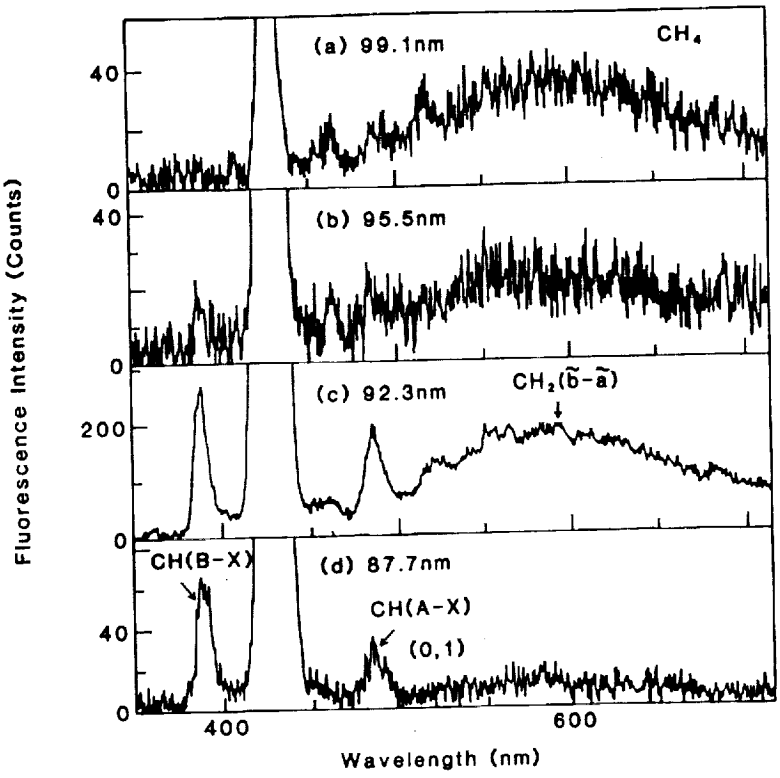

Fig. 3. Amplified fluorescence spectra of CH_4 that show the weak emission systems of $CH(A \rightarrow X)$ (0, 1), $CH(B \rightarrow X)$ (0, 0), and $CH_2(\tilde{b} \rightarrow \tilde{a})$.

$CH(A \rightarrow X)$ (0, 1), $CH(B \rightarrow X)$ (0, 0) and $CH_2(\tilde{b} \rightarrow \tilde{a})$ systems. The fluorescence intensity observed at 68.5 and 63.7 nm is too weak to be distinguished from the noise level. This weak intensity is consistent with the small fluorescence cross section in the 62–76 nm region as shown in Fig. 1(b). The fluorescence cross sections in the 50–62 nm regions are smaller than those in the 80–100 nm

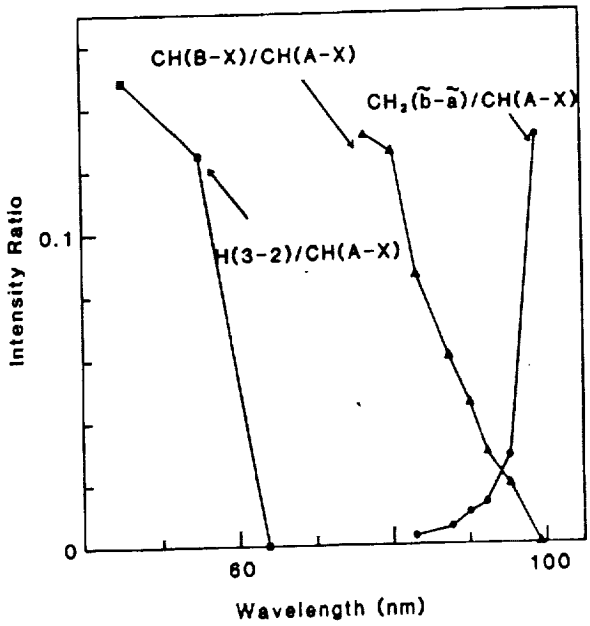

Fig. 4. Ratios of the emission intensities of the $H(n = 3 \rightarrow 2)$, $CH(B \rightarrow X)$ and $CH_2(\tilde{b} \rightarrow \tilde{a})$ systems relative to the $CH(A \rightarrow X)$ (0, 0) system measured at various wavelengths. The data points are joined by lines for eyeguide.

Table 1. Energy and wavelength thresholds for processes of CH_4 relevant to the observed emitting photofragments.

Process	Energy (eV)	Wavelength (nm)
$CH_2(\tilde{a}) + H_2$	5.10	243.1
$CH_2(\tilde{b}) + H_2$	5.98	207.3
$CH + H_2 + H$	9.19	134.9
$CH_2(\tilde{b}) + 2H$	10.50	118.1
$CH(A) + H_2 + H$	12.06	102.8
$CH(B) + H_2 + H$	12.41	99.9
$CH(A) + 3H$	16.58	74.8
$CH(B) + 3H$	16.93	73.2
$CH_3 + H(3)$	16.64	74.5
$CH_3 + H(4)$	17.30	71.7
$CH_3 + H(5)$	17.61	70.4

region by more than one order of magnitude. The atomic $H(2\rightarrow1)$ emission was observed in the 50–62 nm region by Wu and Judge.[4] The intensity ratios of the $CH_2(\tilde{b}\rightarrow\tilde{a})$, $CH(B\rightarrow X)$, and $H(n=3\rightarrow2)$ emissions to $CH(A\rightarrow X)$ are shown in Fig. 4. The ratios provide the information for the emission thresholds, that is, the $CH_2(\tilde{b}\rightarrow\tilde{a})$ emission ends at about 80 nm, and the $H(3\rightarrow2)$ emission starts at about 62 nm.

The fluorescence data are useful for studying the photodissociation process of CH_4. The energy and wavelength thresholds for the production of the emitting photofragments are listed in Table 1. The thresholds are calculated from the heats of formulation[13] and the electronic excitation energies of $CH(A, B)$,[14] $CH_2(\tilde{b})$,[15] and $H(n)$.[16] The $CH_2(\tilde{b}\rightarrow\tilde{a})$ emission observed at wavelengths longer than 107 nm is produced by the $CH_2(\tilde{b}) + H_2$ process, of which the threshold is calculated to be at 207.3 nm. The $CH_2(\tilde{b}) + 2H$ process, which has a threshold wavelength of 118.1 nm, may have a contribution in the 80–100 nm region. The $CH(A\rightarrow X)$ emission is observed at 99.1 nm, but not at 103.7 nm. Since the threshold (102.8 nm) for the process of $CH(A) + H_2 + H$ process is in between these two wavelengths, this process is likely responsible for the emission. The $CH(B\rightarrow X)$ emission that starts to appear at 99.1 nm is likely produced by the $CH(B) + H_2 - H$ process with a threshold at 99.9 nm. The $CH(A, B\rightarrow X)$ emissions observed in the 78–100 nm excitation band are definitely not produced by the $CH(A, B) + 3H$ process, because the threshold energies of these processes are higher than the excitation photon energies. The $CH(A, B) + 3H$ processes may be responsible for the emission observed in the 52–63 nm excitation band. The $H(n \geqslant 3\rightarrow2)$ emissions observed in this excitation band are produced by the $CH_3 + H(n \geqslant 3)$ process.

CH_3OH

The absorption cross section, fluorescence cross section, and fluorescence quantum yield of CH_3OH are shown in Figs. 5(a)–(c), respectively. The absorption cross section measured before 1979 has been summarized by Berkowitz.[11] The current data are about the mean of the existing data that are quite scattered. In contrast to CH_4, the fluorescence of CH_3OH is not well studied. Vinagradov and Vilesov[6] observed fluorescence from photoexcitation of this molecule in the 86–143 nm region, and they attributed the fluorescence to the $OH(A\rightarrow X)$ system with a maximum yield of 0.7% at 88 nm. The current fluorescence yield is close to the earlier data[5] at 86–98 nm, but larger by about a factor of 2 at 98–106 nm. Because of the high experimental uncertainty inherent in the measurement of small fluorescence yield, the agreement is considered to be satisfactory.

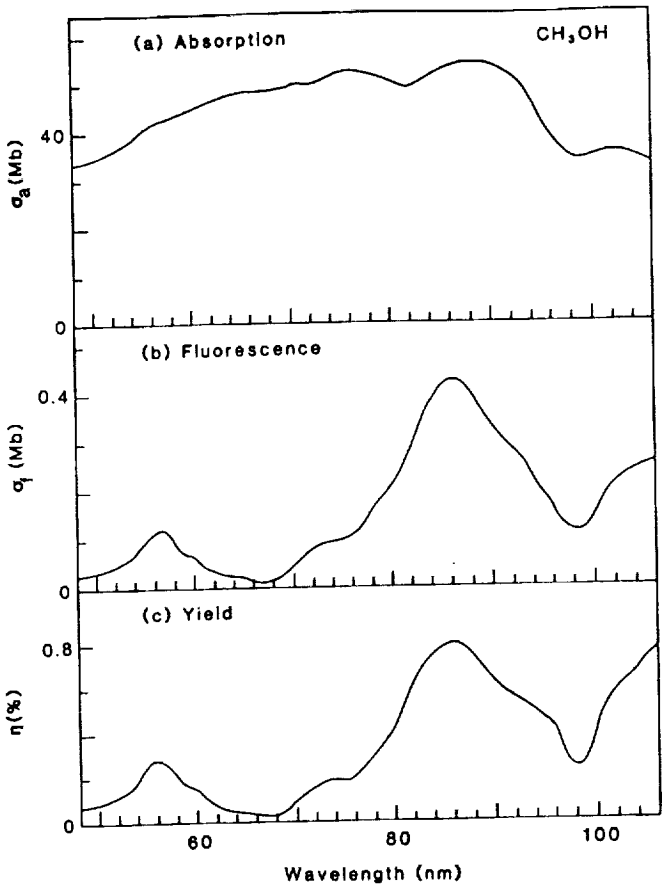

Fig. 5. Same as Fig. 1, except for CH_3OH at 48–106 nm.

The fluorescence cross section shows two excitation bands in the 50–68 and 68–100 nm regions. The fluorescence spectra at 103.7, 99.1, 92.3, 83.4, and 76.5 nm are shown in Figs. 6(a)–(e), respectively. The emission consists of the $OH(A \rightarrow X)$ and $CH(A, B \rightarrow X)$ systems. The fluorescence spectra at 68.5, 63.7, 55.1, and 45.7 nm are shown in Figs. 7(a)–(d), respectively. Relative to the $CH(A, B \rightarrow X)$ emission, the $OH(A \rightarrow X)$ emission system becomes weak at these wavelengths. The $H(n \geq 3 \rightarrow 2)$ emission starts to appear at 63.7 nm, and the intensity becomes stronger at the shorter wavelength.

The energy and wavelength thresholds for the production of the emitting species are listed in Table 2. The threshold energies are calculated from the heats of formation[13,17,18] and the electronic energies of the excited species.[14,15] The $OH(A \rightarrow X)$ emission starts to appear at 147 nm[7] and continues to the shorter wavelengths as shown in Figs. 6 and 7. The $OH(A \rightarrow X)$ intensity decreases with decreasing excitation wavelength. The $CH(A \rightarrow X)$ emission starts to appear at 99.1 nm. This emission can be produced by the dissociative excitation processes of $CH(A) + H + H_2O$ and $CH(A) + H_2 + OH$ with thresholds of 113.2 and 106.9 nm, respectively. By comparison with the photoexcitation process of CH_4, the $CH(A) + H_2 + OH$ process is more favorable. The $CH(A \rightarrow X)$ emission intensity increases with decreasing excitation wavelength. The intensity ratio of the $CH(A \rightarrow X)/OH(A \rightarrow X)$ emissions is shown in Fig. 8. The ratio increases largely toward the short wavelength, indicating that the excitation band in the 70–90 nm region mainly consists of the $CH(A \rightarrow X)$ emission.

As shown in Fig. 7, the $H(n = 3 \rightarrow 2)$ emission appears at 63.7 nm, but not at 68.5 nm. The $H(n = 3)$ can be produced by the process of $CH_2OH + H(3)$ and $CH_3O + H(3)$. of which the threshold wavelengths are 76.7 and 70.7 nm respectively. The $H(n \geq 3 \rightarrow 2)$ systems have emission intensities comparable with $CH(A \rightarrow X)$. The intensity of $H(3 \rightarrow 2)/CH(A \rightarrow X)$ is shown in Fig. 8. The fluorescence spectra at 63.7 and 45.7 nm show a background emission in the 380–520 nm

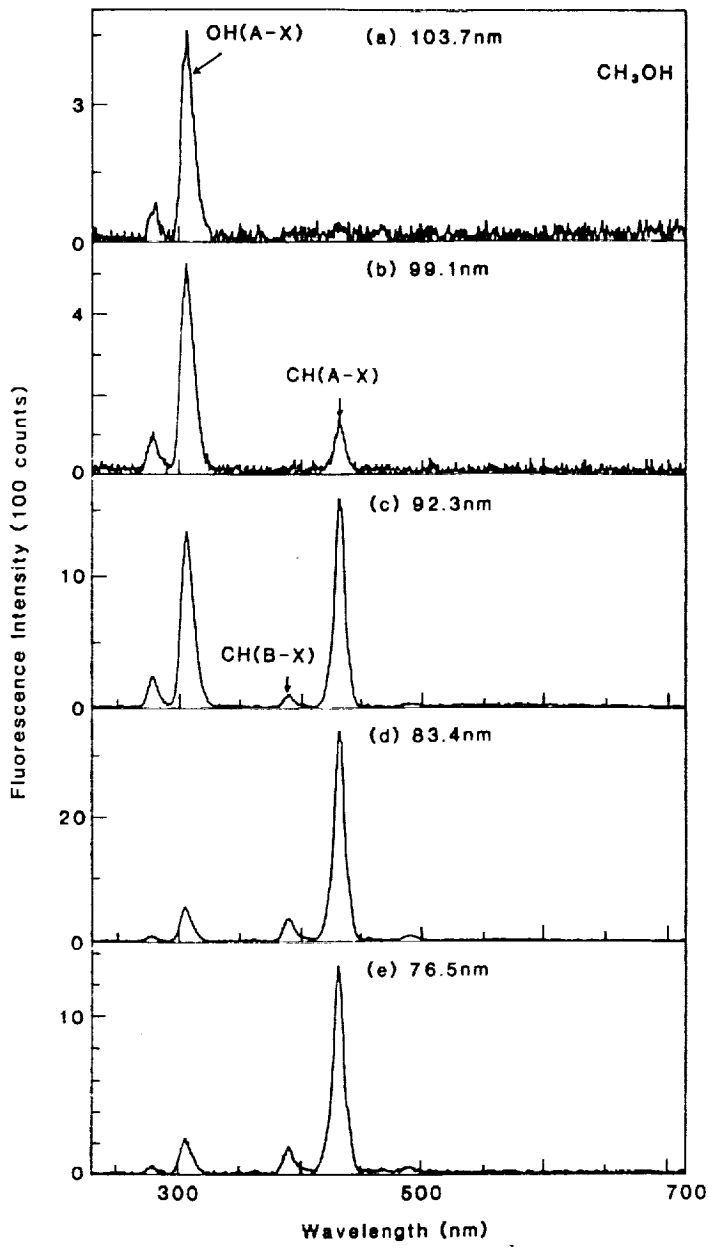

Fig. 6. Fluorescence spectra by photoexcitation of CH_3OH at 103.7–76.5 nm. The emission bands of $CH(A, B \rightarrow X)$ and $OH(A \rightarrow X)$ are indicated.

region, which could be the $CO^+(B \rightarrow X)$ system. This emission may be produced by the process of $CO^+(A) + 2H_2$ and $CO^+(A) + 2H + H_2$, of which the thresholds are 70.6 and 56.1 nm, respectively.

The CH_2^+, CHO^+, CH_3^+, CH_2O^+, and CH_3OH^+ ions have been observed[19] from photoionization of CH_3OH in the 60–110 nm region. The photon energy in the current measurement is sufficient to produce these ions in the excited states that may subsequently emit. The possible emissions from these ions are not observed in the current experiment, indicating that these ions may not emit. Electron-impact excitation[20,21] of CH_3OH also produces emissions from the excited $OH(A)$, $CH(A, B)$, $H(n)$ and $CO^+(A, B)$, but not excited ions. Two-photon excitation of CH_3OH by two ArF (193 nm) laser photons produces only the $CH(A, B \rightarrow X)$ emissions.[22]

CH_3SH

The absorption cross section, fluorescence cross section, and quantum yield of CH_3SH are shown in Figs. 9(a)–(c), respectively. The fluorescence cross section is very small, thus, the uncertainty

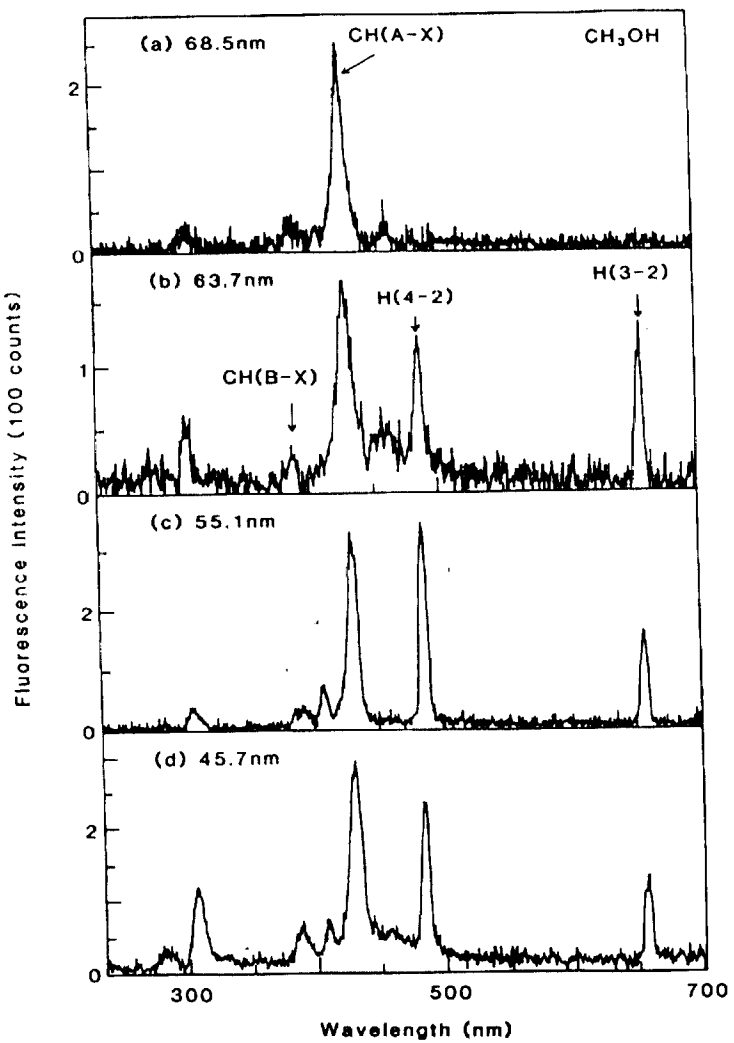

Fig. 7. Fluorescence spectra by photoexcitation of CH_3OH at 68.5-45.7 nm. The identifications of the emission bands are indicated.

Table 2. Energy and wavelength thresholds for photoexcitation processes of CH_3OH relevant to the observed emitting photofragments.

Process	Energy (eV)	Wavelength (nm)
CH_3 + OH	4.08	303.8
CH_3 + OH(A)	8.13	152.4
$CH_2(\tilde{b})$ + H + OH	9.95	124.6
CH(A) + H + H_2O	10.95	113.2
CH(B) + H + H_2O	11.30	109.8
CH(A) + H_2 + OH	11.60	106.9
CH(B) + H_2 + OH	11.95	103.8
CH(X) + H_2 + OH(A)	12.75	97.3
CH(A) + 2H + OH	16.11	76.9
CH_2OH + H(3)	16.18	76.7
CH_3O + H(3)	16.51	75.1
CH_2OH + H(4)	16.84	73.6
CH_3O + H(4)	17.18	72.2
CH_2O + H + H(3)	17.53	70.7
CH_2O + H + H(4)	18.20	68.1
CH_2O + H + H(5)	18.50	67.0
$CO^+(A)$ + $2H_2$	17.57	70.6
$CO^+(A)$ + 2H + H_2	22.08	56.1

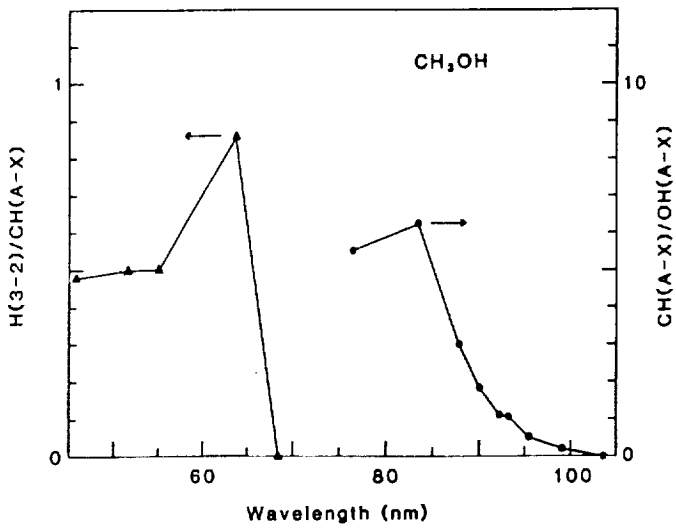

Fig. 8. Intensity ratios of the $H(n = 3 \rightarrow 2)/CH(A \rightarrow X)$ and the $CH(A \rightarrow X)/OH(A \rightarrow X)$ emission systems.

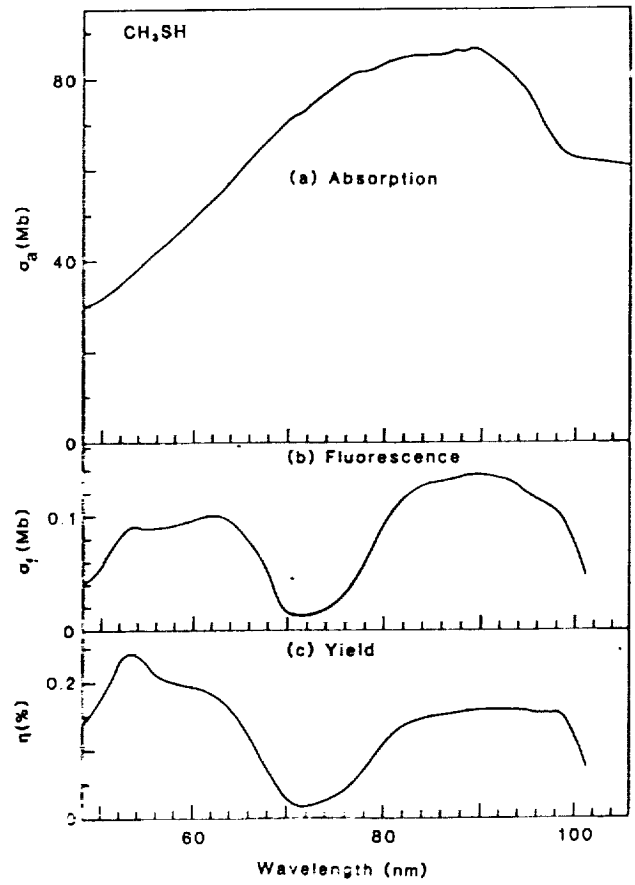

Fig. 9. Same as Fig. 1, except for CH_3SH at 48–106 nm.

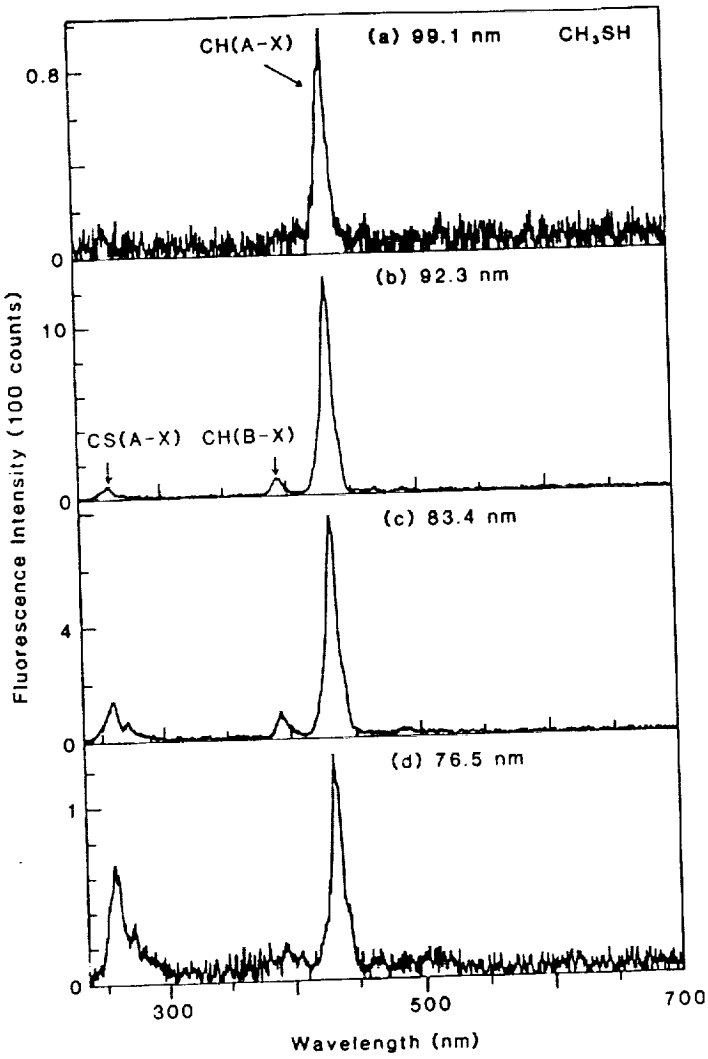

Fig. 10. Fluorescence spectra by photoexcitation of CH_3SH at 99.1–76.5 nm. The emission bands of $CH(A, B \rightarrow X)$ and $CS(A \rightarrow S)$ are indicated.

could be as high as a factor of 2. To the authors knowledge, there are no existing data to compare with the current results.

Similar to CH_4 and CH_3OH, there are two fluorescence excitation bands in the 50–72 and 72–100 nm regions. The fluorescence spectra produced at 99.1, 92.3, 83.4, and 76.5 nm are shown in Figs. 10(a)–(d), respectively. The spectra consist of the $CH(A, B \rightarrow X)$ and $CS(A \rightarrow X)$ systems. The $CS(A \rightarrow X)$ emission is confirmed by comparison with the fluorescence spectra from the vuv excitation[23] of CS_2 and OCS that were observed by the same detection system. The fluorescence spectra produced at 70.0, 63.7, 55.1 and 45.7 nm are shown in Figs. 11(a)–(d), respectively. In addition to the CH* and CS* emission, the $H(n \geqslant 3 \rightarrow 2)$ lines are also observed at these excitation wavelengths.

The energy and wavelength thresholds for the photoexcitation processes that produce the observed emissions are listed in Table 3, which are calculated from the heats of formation[13,17,18] and electronic energies[14,16] of the excited photofragments. The $CH(A \rightarrow X)$ emission appears at 99.1 nm, but not at 103.7 nm. This emission is most likely produced by the dissociative excitation process of $CH(A) + H_2 + SH$ and/or $CH(A) + H + H_2S$, of which the thresholds are 115.8 and 109.6 nm, respectively. The $CH(B \rightarrow X)$ emission is produced by the same process. The $CS(A \rightarrow X)$ emission starts to appear at 99.1 nm. This emission is likely produced by the $CS(A) + 2H + H_2$ process, of which the threshold is 99.4 nm. The $CS(A \rightarrow X)$ emission intensity increases with decreasing

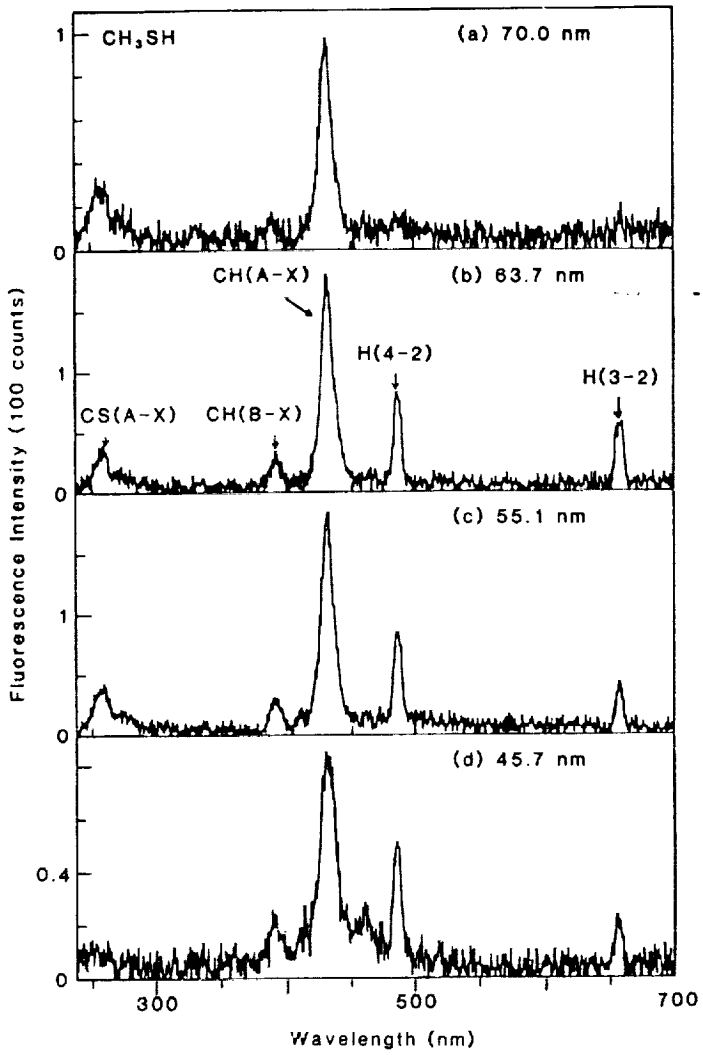

Fig. 11. Fluorescence spectra by photoexcitation of CH_3SH at 70.0–45.7 nm.

Table 3. Energy and wavelength thresholds for photoexcitation processes of CH_3SH relevant to the observed emitting photofragments.

Process	Energy (eV)	Wavelength (nm)
CH_3 + SH(A)	6.99	177.3
CH(A) + H_2 + SH	10.71	115.8
CH(3) + H_2 + SH	11.06	112.1
CH(A) + H + H_2S	11.31	109.6
CH(3) + H + H_2S	11.66	106.3
CS(A) + H_2 + 2H	12.47	99.4
CH_3S + H(3)	16.00	77.5
CH_3S + H(4)	16.66	74.4
CS(A) + 4H	16.99	73.0
CH_2 + SH + H(3)	20.04	61.8
CH_2 + SH + H(4)	20.70	59.9

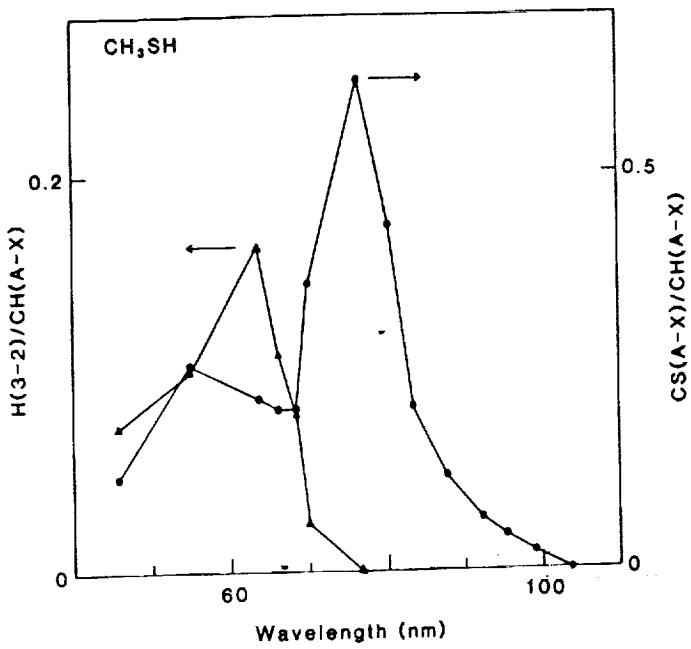

Fig. 12. Intensity ratios of $H(n=3\rightarrow2)/CH(A\rightarrow X)$ and $CS(A\rightarrow X)/CH(A\rightarrow X)$.

excitation wavelength. The intensity ratios of $CS(A\rightarrow X)/CH(A\rightarrow X)$ at various wavelengths are shown in Fig. 12. The $H(n\geqslant 3\rightarrow 2)$ emissions start to appear at 70.0 nm. The $H(3\rightarrow 2)$ emission is likely produced by the $CH_3S + H(3)$ process, of which the threshold is 77.5 nm. The intensity ratios of $H(n=3\rightarrow2)/CH(A\rightarrow X)$ are shown in Fig. 12.

Emissions from the excited $H(n)$, $CH(A, B)$, and $CS(A)$ have been observed from the electron-impact excitation[24] of CH_3SH. The $CH_3S(A\rightarrow X)$ emission in the 380–520 nm region has been observed from photoexcitation of CH_3SH in the 130–175 nm region.[8,25] However, the cross section for this emission is so small (estimated to be $<10^{-20}$ cm^2) that it is not noticeable in the fluorescence spectrum. The SH photofragment could be excited in the A state, but it decays mainly through predissociation[26] so that the expected $SH(A\rightarrow X)$ emission [similar to $OH(A\rightarrow X)$] is not observed. Photoexcitation of CH_3SH in the current wavelength region could produce ions[27] (such as CH_3SH^+, CH_3S^+, etc.) in the excited states; however, emissions from these ions were not observed.

CONCLUSIONS

The photoabsorption and fluorescence cross sections of CH_4, CH_3OH, and CH_3SH were measured in the extreme u.v. region. All three molecules show two fluorescence excitation bands—one at 50–65 nm and the other at 75–100 nm. The $H(n\rightarrow2)$ and $CH(A, B\rightarrow X)$ emissions are commonly observed in all three molecules. In addition, the $CH_2(\tilde{b}\rightarrow\tilde{a})$ emission is observed from CH_4, $OH(A\rightarrow X)$ from CH_3OH, and $CS(A\rightarrow X)$ from CH_3SH. The CH and CS emissions are produced by dissociation of multiple bonds; further study of these photoexcitation processes is of interest.

Acknowledgements—This report is based on the work supported by NASA and NSF. The synchrotron radiation facility at the University of Wisconsin is supported by NSF.

REFERENCES

1. P. H. Metzger and G. R. Cook, *J. Chem. Phys.* **41**, 642 (1964).
2. A. R. Welch and D. L. Judge, *J. Chem. Phys.* **57**, 286 (1972).
3. L. C. Lee, E. Phillips, and D. L. Judge, *J. Chem. Phys.* **67**, 1237 (1977).
4. C. Y. R. Wu and D. L. Judge, *J. Chem. Phys.* **75**, 172 (1981).
5. L. C. Lee and C. C. Chiang, *J. Chem. Phys.* **78**, 688 (1983).
6. I. P. Vinogradov and F. I. Vilesov, *Khim. Vys. Energ.* **11**, 25 (1977).

7. J. B. Nee, M. Suto, and L. C. Lee, *Chem. Phys.* **98,** 147 (1985).
8. I. Tokue, A. Hiraya, and K. Shobatake, *Chem. Phys.* **116,** 449 (1987).
9. L. C. Lee and M. Suto, *Chem. Phys.* **110,** 161 (1986); L. C. Lee, *J. Chem. Phys.* **72,** 4334 (1980).
10. L. C. Lee, J. C. Han, C. Ye, and M. Suto, *J. Chem. Phys.* **92,** 133 (1990).
11. J. Berkowitz, *Photoabsorption, Photoionization, and Photoelectron Spectroscopy*, Academic Press, New York, NY (1979).
12. J. A. R. Samson and G. Haddad, Data published in the review paper by J. W. Gallagher, C. E. Brion, J. A. R. Samson, and P. W. Langoff, *J. Phys. Chem. Ref. Data* **17,** 9 (1988).
13. M. W. Chase, Jr., C. A. Davies, J. R. Dwoney, Jr., D. J. Frurip, R. A. McDonald, and A. N. Syverud, *J. Phys. Chem. Ref. Data* **14,** Suppl. No. 1 (1985).
14. K. P. Huber and G. Herzberg, *Constants of Diatomic Molecules*, Van Nostrand-Reinhold, New York, NY (1979).
15. G. Herzberg and J. W. C. Johns, *Proc. R. Soc. (Lond.)* **A295,** 107 (1966).
16. C. E. Moore, "Atomic Energy Levels," *NSRDS-NBS 35*, National Bureau Standards, Washington, DC (1971).
17. S. W. Benson, *Thermochemical Kinetics*, Wiley, New York, NY (1976).
18. H. Okabe, *Photochemistry of Small Molecules*, Wiley, New York, NY (1978).
19. J. Berkowitz, *J. Chem. Phys.* **69,** 3044 (1978).
20. D. E. Donahue, J. A. Schiavone, and R. S. Freund, *J. Chem. Phys.* **67,** 769 (1977).
21. T. Ogawa, S. Ishibashi, and H. Kawazumi, *J. Phys. Chem.* **88,** 1662 (1984).
22. C. Fotakis, M. Martin, K. P. Lawley, and R. J. Donavan, *Chem. Phys. Lett.* **67,** 1 (1979).
23. L. C. Lee and D. L. Judge, *J. Chem. Phys.* **63,** 2782 (1975).
24. M. Toyoda, T. Ogawa., and N. Ishibashi, *Bull. Chem. Soc. Japan* **47,** 95 (1974).
25. K. Ohbayashi, H. Akimoto, and I. Tanaka, *Chem. Phys. Lett.* **52,** 47 (1977).
26. L. C. Lee, X. Wang, and M. Suto, *J. Chem. Phys.* **86,** 4353 (1987).
27. R. E. Kutina, A. K. Edwards, G. L. Goodman, and J. Berkowitz, *J. Chem. Phys.* 77, 5508 (1982).